Updates to the MAX IV 3 GeV Storage Ring Lattice

Simon C. Leemann

January 17, 2011 (updated June 12, 2012)

MAX-lab Internal Note 20110117[1]

Abstract

The optics for the MAX IV 3 GeV storage ring have been modified and the official lattice has been updated. The new 20110117 branch [1] will replace the previous 20101101 branch. The optics change has resulted from the requirement to match to a greater number of strong IDs than originally foreseen as well as operational concerns regarding powering of the pole-face strips (PFSs). Additionally, a new matching method is applied so that the powering of PFSs in the dipoles does not need to be varied whenever strong ID gaps change. Although it appears only minor changes to the linear optics were applied, the vertical tune has been shifted by two integers which entails a significant change of vertical chromaticity and hence modifications in the nonlinear correction scheme. This document describes the linear and nonlinear optics changes, presents the new ID matching technique and required tuning range, and summarizes all other modifications to the official lattice. A list of current official lattice files and their purpose is appended.

1 Motivation Behind the Optics Change

Initial measurements of the prototype matching cell showed that exciting the PFSs generates, aside from the desired gradient, a considerable dipole kick [2]. This dipole kick would in itself not present a problem if the PFS powering were static; in such a case the dipole strength could be adjusted and any residual error compensated by the orbit correctors. Since the PFSs were however to be adjusted frequently (as a

[1] This document can be found at `http://www.maxlab.lu.se/node/999`

result of continuously varying gaps in strong IDs during standard user operation), this dipole component becomes a frequently-varying perturbation which cannot be easily compensated for.

It was also noticed that each strong ID (e.g. the 3 m long IVU used in the DDR [3]) would require the PFSs to be powered so as to adjust the dipole gradient by about 0.2% for compensation of a fully closed gap. Since we expect roughly ten such devices to be operated in the MAX IV 3 GeV ring, we have to conclude that the PFSs need to be able to vary the overall gradient by several percent (this includes restoring the design working point in the actual machine, possibly from a biased design gradient). Such a large gradient change is beyond what air-cooled PFSs that fit between the dipole yoke and the vacuum chamber can deliver. We can thus envisage a situation where we could not bring further strong IDs online because of lack of optics tuning range. This is of course a highly undesirable situation.

The problem of the large required gradient tuning range was compounded by considerations regarding the type of power supply to drive PFS current. Unless a significant gradient bias was applied to the design optics, a bipolar power supply capable of supplying very large currents was going to be required. Such power supplies are rare and expensive. In fact, even if one were to buy an expensive high-current bipolar power supply, we have to expect that the optics will be tuned, during at least some of the time, close to the zero crossing of the power supply. Since such high-current bipolar power supplies are often implemented internally as switched unipolar power supplies, tuning close to the zero crossing is inherently connected to delayed response and/or stability issues. Keeping in mind that such tuning could occur constantly to follow several independently varying ID gaps, such a situation is also deemed highly undesirable.

2 Strategy

As a consequence of the issues mentioned above it was decided to embrace a new optics which would be less sensitive to strong IDs. Accordingly, optics matching to the IDs could then be done exclusively by varying the quadrupole doublets in the long straights. The PFSs would only be powered in order to set the desired working point, i.e. in a static way[2]. Furthermore, the overall defocusing gradient in the dipoles could be biased with respect to the design optics, so that adjustments made in the actual machine after installation and beyond, can be made by powering the PFSs in a unipolar fashion. This would allow use of a less expensive but more stable and lower-latency power supply.

The proposed method to decrease sensitivity of the optics to strong IDs is to reduce the vertical beta function in the long straights since the tune shift generated by the ID scales linearly with the average beta function value in the ID [3]. This has another beneficial effect: the same diffraction-limited beam size can be achieved at more relaxed levels of betatron coupling (possibly higher lifetime). Or conversely, at the same level of betatron coupling (i.e. without reducing lifetime), the vertical source size in the ID is now reduced. It had been previously established, that reducing the vertical beam size would improve matching to the photon beam emerging from the ID.

We have decided to reduce the vertical beam size from the previous $\beta_y^* = 4.8\,\mathrm{m}$ to a new value of $\beta_y^* = 2.0\,\mathrm{m}$ (where the asterisk * indicates values at the center of the long straight). This in turn reduces the vertical beam size by a factor $\sqrt{2/4.8} = 0.65$ at the center of the ID. If this were done by adjusting all quadrupoles with the boundary condition of keeping the working point at its previous values ($\nu_x = 42.20$, $\nu_y = 14.28$) the vertical beta function values within the achromats would have to rise considerably to compensate for the vertical beta squeeze in the long straights. Since this is not desirable, the new optics are adjusted in such a way that the fractional vertical tune is conserved, however the integer is allowed to increase by two. In this way we end up with beta functions that closely mimic the previous optics within the achromats while retaining the previous working point environment in tune space and similar quadrupole settings.

[2]Because of the static nature of damping wigglers, we can still contemplate use of the PFSs for optics matching to such devices.

3 New Linear Optics

The result of the new optics is shown in Fig. 1. The beta functions have changed almost only in the long straights and in the vertical plane. As a consequence, most of the derived properties (cf. parameters on the right in Fig. 1) remain unchanged. Note however the new working point with vertical tune $\nu_y = 16.28$. The new optics have been designed with OPA and Tracy-3; results derived with the two codes are in agreement. Table 1 shows changes to the focusing gradient strengths applied in the new optics branch.

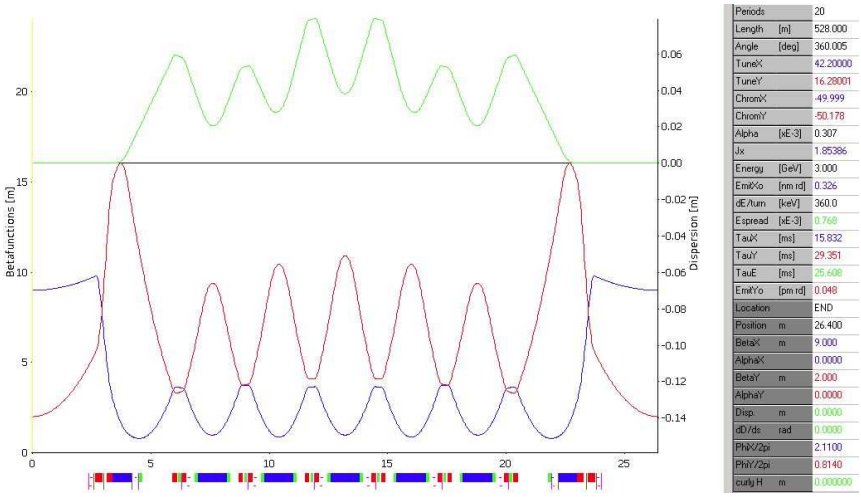

Figure 1: The new optics in one of the 20 achromats of the MAX IV 3 GeV storage ring. The most important derived properties are indicated on the right.

Table 1: List of focusing gradient changes by magnet family. Note that for the dipole gradient the strength is given by a scaling factor. The scaling factor is defined with respect to the dipole model slices as detailed in the DDR [3].

Magnet family	Gradient change	Rel. difference
QD (dipole gradient)	$f = 1.001224 \longrightarrow 0.992047$	-0.92%
QF	$b_2 = 4.037860\,\mathrm{m}^{-2} \longrightarrow 4.030907\,\mathrm{m}^{-2}$	-0.17%
QFm	$b_2 = 3.779900\,\mathrm{m}^{-2} \longrightarrow 3.776156\,\mathrm{m}^{-2}$	-0.10%
QFend	$b_2 = 3.521817\,\mathrm{m}^{-2} \longrightarrow 3.656234\,\mathrm{m}^{-2}$	$+3.82\%$
QDend	$b_2 = -2.176206\,\mathrm{m}^{-2} \longrightarrow -2.507705\,\mathrm{m}^{-2}$	$+15.23\%$

4 New Optics Matching for Strong IDs

With the new optics the matching to strong IDs follows the same "mitigation" strategy detailed in the DDR [3]. The optics are still adjusted to strong IDs both locally and globally. However, the optics matching is performed by varying different magnet families. Since the vertical beta function has been squeezed in the IDs, the defocusing effect of IDs has become much smaller. Consequently it now suffices to adjust only the quadrupole doublet (QDend and QFend) flanking the ID in order to match the beta functions locally to the ID. We use the 3.7 m long permanent-magnet in-vacuum undulator pmuL detailed in [4] as an example since it is the strongest presently foreseen ID in the MAX IV 3 GeV storage ring. The key parameters of this device are summarized in Table 2.

Table 2: Key parameters of the 3.7 m long permanent-magnet in-vacuum undulator pmuL. It is the strongest presently foreseen ID in the MAX IV 3 GeV storage ring.

Period length	18.5 mm
No. of periods	202
Effective magnetic field	1.111 T
Minimum gap	4.2 mm

The optics changes caused by the ID as well as required local matching in the "mitigation" scheme (DDR terminology) are displayed in Table 3. As a result of this matching, the beta functions of the adjacent long straights are matched to those of a bare achromat. This ensures that the ID does not cause a beta beat throughout the rest of the storage ring. When the local matching has been applied, the resulting phase advance has to be corrected to restore the design working point. This is done globally as originally foreseen, but in the new optics it is achieved by varying all focusing doublets in the long straights coherently; the QF quadrupole family and QD (PFSs) are not varied. Table 4 shows the required variation of all doublets around the machine to restore the working point after the changes shown in Table 3 have been applied locally around the ID.

It has been verified that this global working point correction remains applicable when the phase advance, arising from the simultaneous operation of ten or nineteen ("fully loaded ring"') such IDs in the storage ring, has to be corrected. This is displayed in Tables 5 and 6.

Table 3: Adjustments required to match the adjacent achromats to the 3.7 m long pmuL installed in the long straight section of the MAX IV 3 GeV storage ring. The relevant change is the increase in defocusing magnet strength (+0.5% here) to reduce vertical beam size within the ID.

Before local adjustment		After local adjustment	
QFend @ pmuL: $b_2 = 3.656234\,\mathrm{m}^{-2}$	$\longrightarrow$	$3.660407\,\mathrm{m}^{-2}$	$(+0.11\%)$
QDend @ pmuL: $b_2 = -2.507705\,\mathrm{m}^{-2}$	$\longrightarrow$	$-2.519325\,\mathrm{m}^{-2}$	$(+0.46\%)$
$\Downarrow$		$\Downarrow$	
$\beta_x^* = 9.000\,\mathrm{m}$	$\longrightarrow$	$9.000\,\mathrm{m}$	
$\beta_y^* = 2.044\,\mathrm{m}$	$\longrightarrow$	$2.000\,\mathrm{m}$	
	but also:		
		$\Delta\nu_x < -0.0001$	
		$\Delta\nu_y = +0.0099$	

Table 4: Adjustments required to re-establish the original working point after insertion of a single 3.7 m long pmuL in the MAX IV 3 GeV storage ring. The largest change is the compensation of an excess 0.05% vertical phase advance.

Before global adjustment		After global adjustment	
all QFend: $b_2 = 3.656234\,\mathrm{m}^{-2}$	$\longrightarrow$	$3.655791\,\mathrm{m}^{-2}$	(-0.01%)
all QDend: $b_2 = -2.507705\,\mathrm{m}^{-2}$	$\longrightarrow$	$-2.506546\,\mathrm{m}^{-2}$	(-0.05%)
$\Downarrow$		$\Downarrow$	
$\Delta\nu_x < -0.0001$	$\longrightarrow$	$\nu_x = 42.200$	
$\Delta\nu_y = +0.0099$	$\longrightarrow$	$\nu_y = 16.280$	
	leaving:		
		$\beta_x^* = 8.999\,\mathrm{m}$	(-0.01%)
		$\beta_y^* = 2.005\,\mathrm{m}$	$(+0.25\%)$

Table 5: Adjustments required to re-establish the original working point after insertion of ten 3.7 m long pmuL in the MAX IV 3 GeV storage ring. The largest change is the compensation of an excess 0.6% vertical phase advance.

Before global adjustment		After global adjustment	
all QFend: $b_2 = 3.656234\,\mathrm{m}^{-2}$	$\longrightarrow$	$3.647719\,\mathrm{m}^{-2}$	(-0.24%)
all QDend: $b_2 = -2.507705\,\mathrm{m}^{-2}$	$\longrightarrow$	$-2.485508\,\mathrm{m}^{-2}$	(-0.86%)
$\Downarrow$		$\Downarrow$	
$\Delta\nu_x = -0.00211$	$\longrightarrow$	$\nu_x = 42.200$	
$\Delta\nu_y = +0.09904$	$\longrightarrow$	$\nu_y = 16.280$	
	leaving:		
		$\beta_x^* = 8.972\,\mathrm{m}$	(-0.3%)
		$\beta_y^* = 2.066\,\mathrm{m}$	$(+3.3\%)$

Table 6: Adjustments required to re-establish the original working point after insertion of nineteen 3.7 m long pmuL in the MAX IV 3 GeV storage ring. The largest change is the compensation of an excess 0.56% vertical phase advance.

Before adjustments		After adjustments	
QFend @ pmuL: $b_2 = 3.656234\,\mathrm{m}^{-2}$	$\longrightarrow$	$3.651824\,\mathrm{m}^{-2}$	(-0.12%)
QDend @ pmuL: $b_2 = -2.507705\,\mathrm{m}^{-2}$	$\longrightarrow$	$-2.496936\,\mathrm{m}^{-2}$	(-0.43%)
all QFend: $b_2 = 3.656234\,\mathrm{m}^{-2}$	$\longrightarrow$	$3.656234\,\mathrm{m}^{-2}$	(0.00%)
all QDend: $b_2 = -2.507705\,\mathrm{m}^{-2}$	$\longrightarrow$	$-2.507705\,\mathrm{m}^{-2}$	(0.00%)
$\Downarrow$		$\Downarrow$	
$\Delta\nu_x < 0.00001$	$\longrightarrow$	$\nu_x = 42.200$	
$\Delta\nu_y = +0.08841$	$\longrightarrow$	$\nu_y = 16.280$	
	leaving:		
		$\beta_x^* = 9.008\,\mathrm{m}$	$(< 0.1\%)$
		$\beta_y^* = 2.014\,\mathrm{m}$	$(+0.7\%)$

We note finally, that in the case of four 2 m or two 4 m PMDWs of the type used in the DDR, the optics can also be matched to the PMDW in the above detailed way using only the doublets in the long straights. The defocusing strength of a 2 m PMDW is comparable to the 3.7 m pmuL and hence the required optics matching is of similar magnitude. Since the PMDWs are however static devices they can also be matched in the previous fashion using the PFSs as detailed in the DDR. From a beam dynamics point of view there is very little difference so that the choice of method can be determined by operational and/or budgetary considerations. Table 7 shows matching to two 4 m long PMDWs installed in an otherwise bare lattice; since PMDW matching using the PFSs was already demonstrated in the DDR, the table here shows the matching results when the doublets are used.

Table 7: Adjustments required to match the optics to two 4 m long 2.22 T PMDWs installed in two long straight sections of the MAX IV 3 GeV storage ring (bare lattice).

Before local adjustment		After local adjustment	
QFend @ PMDW: $b_2 = 3.656234\,\mathrm{m}^{-2}$	$\longrightarrow$	$3.668802\,\mathrm{m}^{-2}$	$(+0.3\%)$
QDend @ PMDW: $b_2 = -2.507705\,\mathrm{m}^{-2}$	$\longrightarrow$	$-2.542735\,\mathrm{m}^{-2}$	$(+1.4\%)$
		$\Downarrow$	
		$\Delta\nu_x = 2 \times -0.0006$	
		$\Delta\nu_y = 2 \times +0.0349$	
Before global adjustment		**After global adjustment**	
all QFend: $b_2 = 3.656234\,\mathrm{m}^{-2}$	$\longrightarrow$	$3.652870\,\mathrm{m}^{-2}$	(-0.09%)
all QDend: $b_2 = -2.507705\,\mathrm{m}^{-2}$	$\longrightarrow$	$-2.499016\,\mathrm{m}^{-2}$	(-0.35%)
	leaving:		
		$\beta_x^* = 8.994\,\mathrm{m}$	(-0.1%)
		$\beta_y^* = 2.033\,\mathrm{m}$	$(+1.7\%)$

5 Changes to the Nonlinear Optics

Despite the moderate changes to the beta functions the vertical tune has been increased considerably. This in turn has increased the natural vertical chromaticity by about 6 units or 14% (cf. Fig. 1). Therefore a new linear chromatic correction becomes necessary. In accordance with the nonlinear optics strategy pursued for MAX IV, this means a new nonlinear optics is required for the new linear optics. The new nonlinear correction derived from the old 410 branch is labeled 420.

Table 8: List of sextupole gradient changes by magnet family. Note the significant increase of required strength on the SDend family.

Magnet family	Sextupole gradient change	Rel. difference
SD	$b_3 = -117.919\,\mathrm{m}^{-3} \longrightarrow -116.414\,\mathrm{m}^{-3}$	-1.3%
SDend	$b_3 = -134.000\,\mathrm{m}^{-3} \longrightarrow -170.000\,\mathrm{m}^{-3}$	$+26.9\%$
SFm	$b_3 = 160.000\,\mathrm{m}^{-3} \longrightarrow 170.000\,\mathrm{m}^{-3}$	$+6.3\%$
SFo	$b_3 = 170.000\,\mathrm{m}^{-3} \longrightarrow 174.000\,\mathrm{m}^{-3}$	$+2.4\%$
SFi	$b_3 = 214.767\,\mathrm{m}^{-3} \longrightarrow 206.707\,\mathrm{m}^{-3}$	-3.8%

As a starting point for the new nonlinear optics the linear chromaticity was again corrected to +1.0 in both planes using the strongest chromatic sextupoles: SFi and SD. All sextupoles were then adjusted to minimize first-order driving terms in the sextupole Hamiltonian, minimize second-order chromaticity, as well as to optimize the overall chromatic tune shift (of course with the boundary condition that linear chromaticity has to remain at +1.0). This optimization was done using SVD and applying the same weights as in the original 410 nonlinear optics branch. Finally, the families were manually tweaked to tailor the proper wrap-up of chromatic tune shift. Table 8 shows the new sextupole settings in the 420 nonlinear optics. The chromatic tune footprint now closely resembles that of the 412 nonlinear optics. Chromaticity is displayed in Fig. 2.

At this point the octupole settings were re-optimized. The original target values for ADTS driving terms in the octupole Hamiltonian were adjusted so as to minimize the ADTS of the new optics within the modified acceptance of the ring. The target values were modified as following: $\partial\nu_x/\partial J_x = +700 \longrightarrow -2500$, $\partial\nu_x/\partial J_y = \partial\nu_y/\partial J_x = +2300$ (no change), and $\partial\nu_y/\partial J_y = +2000 \longrightarrow +3500$. The required octupole gradients to reach these target values (derived using SVD) are displayed in Table 9. The resulting ADTS is low and tightly wrapped up which leads to an overall highly compact tune footprint (cf. Fig. 3).

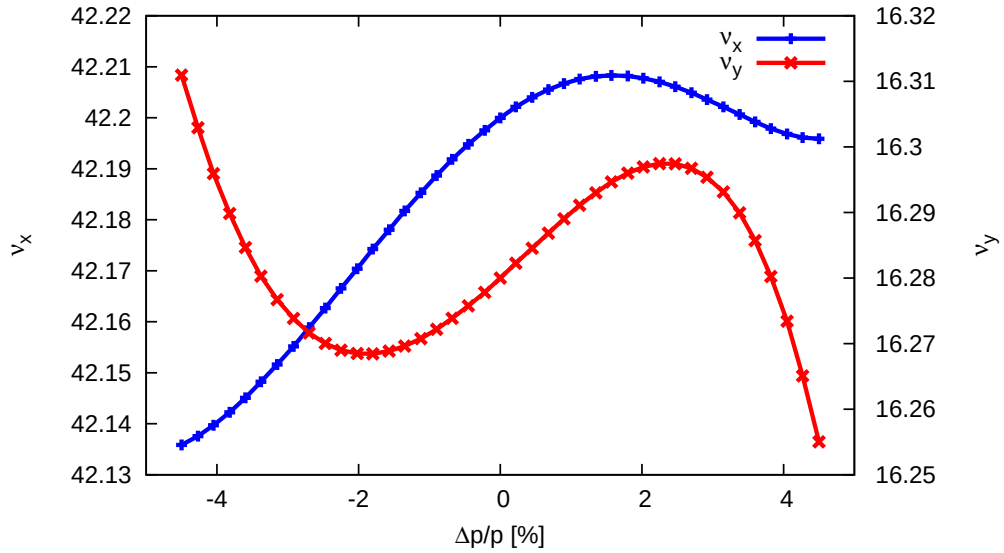

Figure 2: Chromaticity calculated by Tracy-3 using the new sextupole settings of the 420 nonlinear optics branch. The range chosen corresponds to the required MA of the ring.

The result of this small tune footprint is reflected by the large DA (cf. Figs. 4 and 5) as well as large MA (cf. Fig. 6). Four bands can be recognized within the required $\pm 4.5\%$ MA: the skew octupole resonance $2\nu_x + 2\nu_y = 117$ is the cause of the two bands around $\delta = +2\%$. The band around $\delta = -2.5\%$ is caused by $\nu_x + 3\nu_y = 91$, while the band around $\delta = +4\%$ is caused by $4\nu_y = 65$ and $5\nu_x = 211$. The three skew octupole resonances are not expected to be driven strongly. This is of course also the case for the decapole resonance. Compared to the results of the previous 410 nonlinear optics branch we recognize that while DA has reduced slightly, FMA reveals lower diffusion within the required aperture. This is the result of a stronger compression of ADTS in tune space; hence on-momentum particles no longer cross

Table 9: List of octupole gradient changes by magnet family. Note the significant increase of required strength on the OYY family.

Magnet family	Octupole gradient change	Rel. difference
OXX	$b_4 = -1314.266\,\mathrm{m}^{-4} \longrightarrow -1618.313\,\mathrm{m}^{-4}$	+23.1%
OXY	$b_4 = +2181.429\,\mathrm{m}^{-4} \longrightarrow +3250.189\,\mathrm{m}^{-4}$	+49.0%
OYY	$b_4 = -688.567\,\mathrm{m}^{-4} \longrightarrow -1416.590\,\mathrm{m}^{-4}$	+105.7%

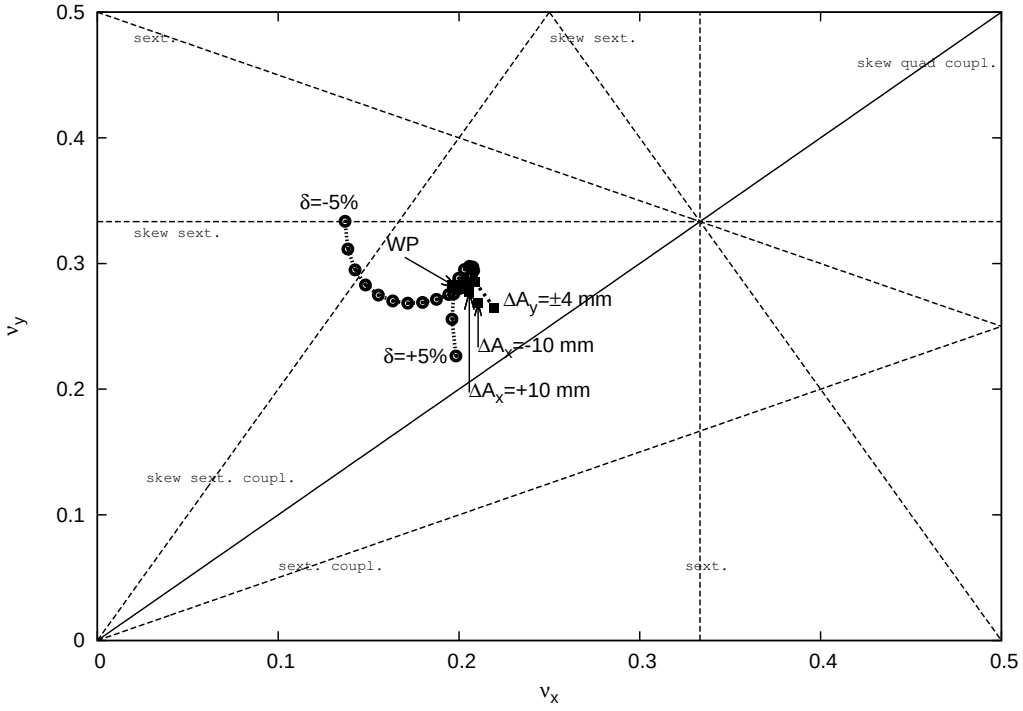

Figure 3: A plot of fractional tune space for the MAX IV 3 GeV storage ring bare lattice as calculated by OPA. Resonance and skew resonance lines have been included up to third order. WP indicates the working point. The step size chosen for the chromatic tune shift is 0.5% and 2.5 mm [1.0 mm] for the horizontal [vertical] amplitude-dependent tune shift.

the skew octupole resonance $2\nu_x + 2\nu_y = 117$. Momentum acceptance appears very similar to the results for the 410 nonlinear optics branch despite the fact that the overall chromatic tune shift now covers more vertical tune space. The similar MA is further corroborated by the Touschek lifetime. OPA estimates for dynamic Touschek lifetime (bare lattice, no Landau cavities, 1% emittance coupling, 1.8 MV total cavity voltage $\rightarrow$ $\delta_{\mathrm{rf}} = 7\%$, 500 mA stored current, IBS neglected) show that the new 420 branch has actually increased Touschek lifetime by 13% compared to the original 410 nonlinear optics. Keeping in mind, that the new optics also allow better matching to the photon beam without further reducing betatron coupling (which would have reduced lifetime), this is a great result.

To give a more complete picture, we investigate the effect of installing ten strong IVUs (of the same type as the 3 m long 1.27 T IVU used in the DDR) in the storage ring and applying the usual linear optics matching. With the same 420 nonlinear

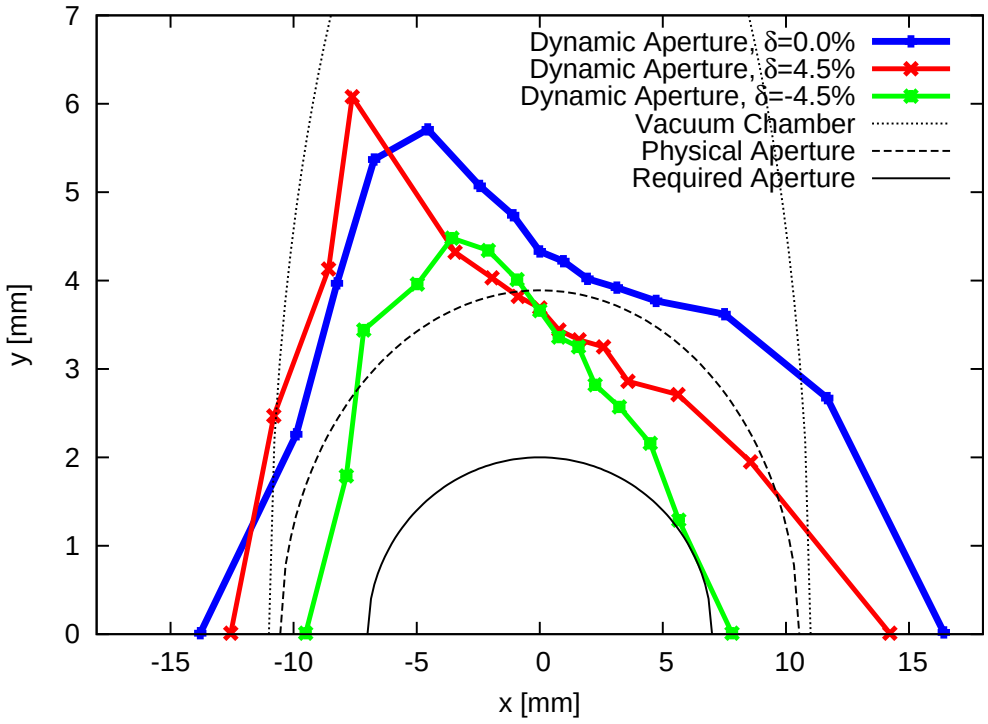

Figure 4: Dynamic aperture at the center of the long straight section in the MAX IV 3 GeV storage ring (bare lattice). Tracking was performed with Tracy-3 in 6D for half a synchrotron period. Physical aperture and acceptance are also indicated in the plot.

optics, the linear chromaticity now drifts slightly from the desired +1.0 setting to $\xi_x = +1.03$ and $\xi_y = +1.24$. This is a rather minor deviation and hence it is of interest to investigate the performance of the ring in this configuration if we assume that no changes are made to the originally set 420 nonlinear optics. The possibility of running with constant nonlinear optics settings is of great advantage during user operation. In user operation, ID gap changes can be frequent and consequently the linear optics will be re-matched constantly. It is fairly complex and rather tedious to also update the nonlinear settings so that they follow the linear optics variations. Instead, if the nonlinear optics can be left constant despite continuous minor changes to the linear optics, operation of the machine becomes significantly less complex.

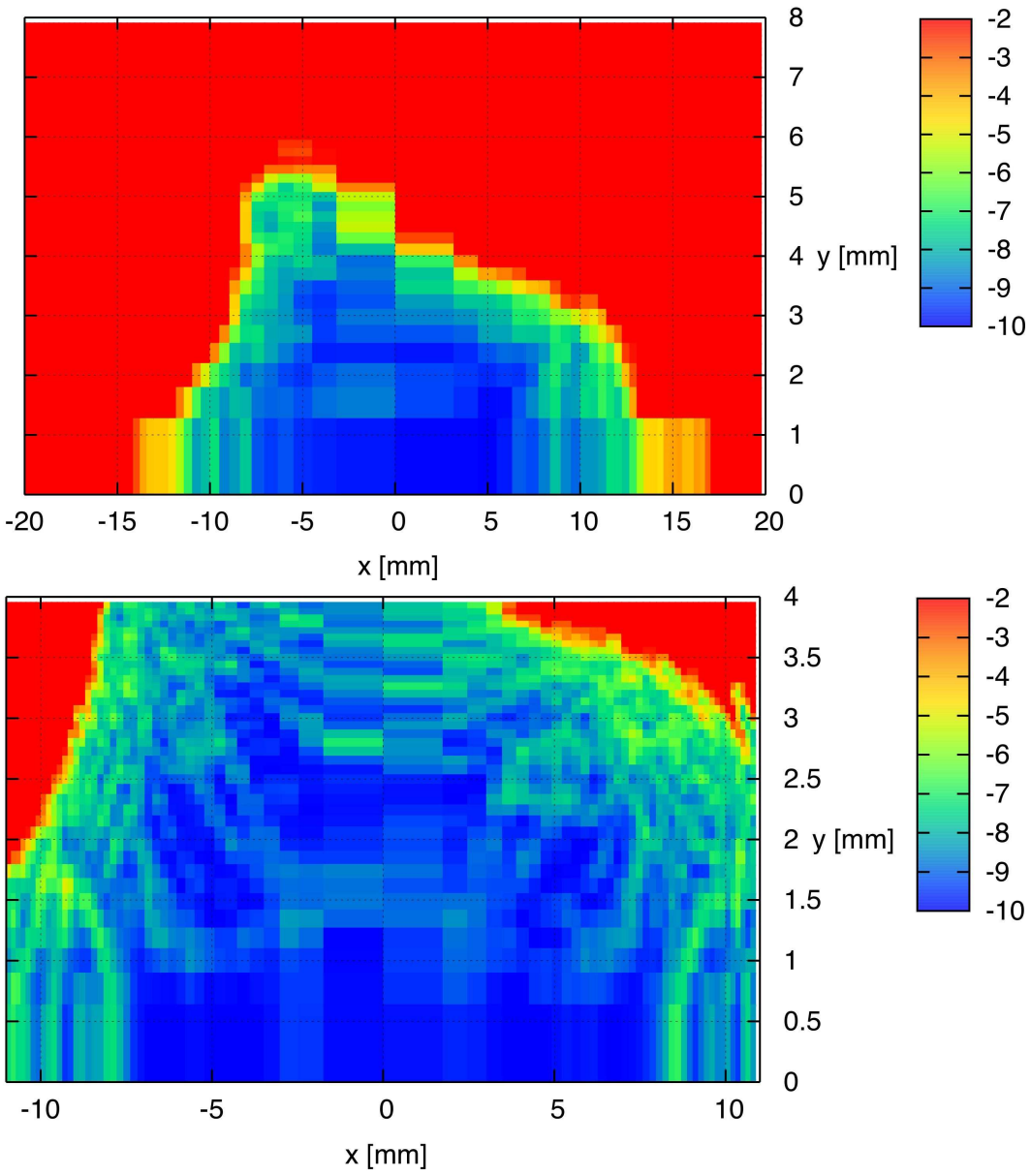

Figure 5: Diffusion maps for the MAX IV 3 GeV storage ring bare lattice taken at the center of the straight section (physical acceptance at this location is $\pm 10.4\,\text{mm} \times \pm 3.9\,\text{mm}$). The lower plot is a magnification of the core area of the upper plot. Blue areas show small tune shifts, red areas show large tune shifts and particle loss. The plots have been generated with Tracy-3 by scanning transverse configuration space on-momentum and tracking for 2048 turns.

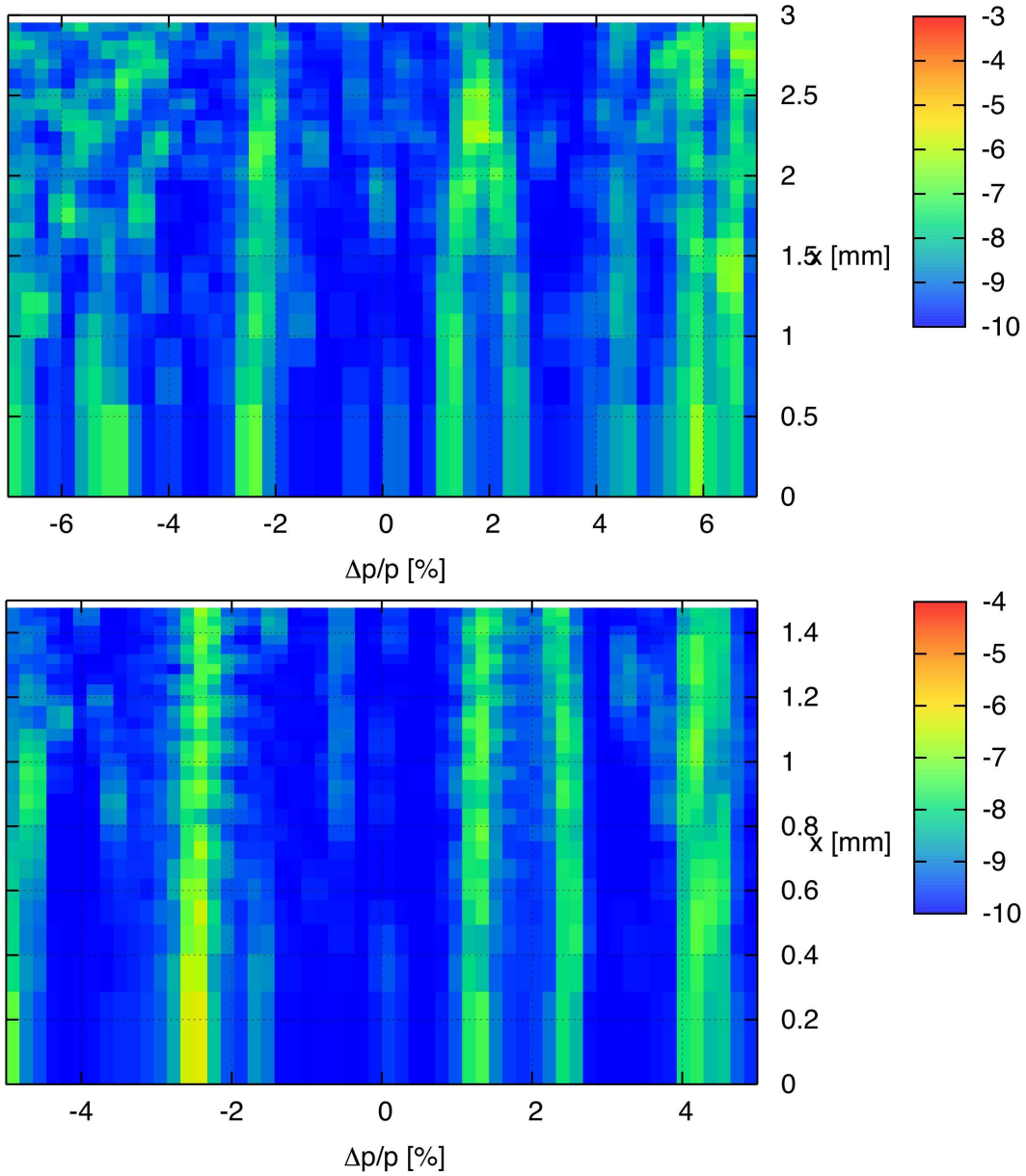

Figure 6: Diffusion maps for the MAX IV 3 GeV storage ring bare lattice taken at the center of the straight section for off-momentum particles. The lower plot is a magnification of the core area of the upper plot. Blue areas show small tune shifts, red areas show large tune shifts and particle loss. The plots have been generated with Tracy-3 by scanning the horizontal coordinate and momenta and tracking for 2048 turns. The initial vertical amplitude was +1 mm.

For this purpose we re-evaluate chromaticity (cf. Fig. 7), tune footprint (cf. Fig. 8), DA (cf. Fig. 9), and FMA (cf. Figs. 10 and 11) for the case of the ring with ten IVUs where the 420 nonlinear optics settings have been left unchanged. Although chromatic behavior is quite similar, the overall vertical chromatic tune shift is actually lower in the loaded ring. Accordingly, the tune footprint of the loaded ring is even smaller than for the bare lattice configuration.

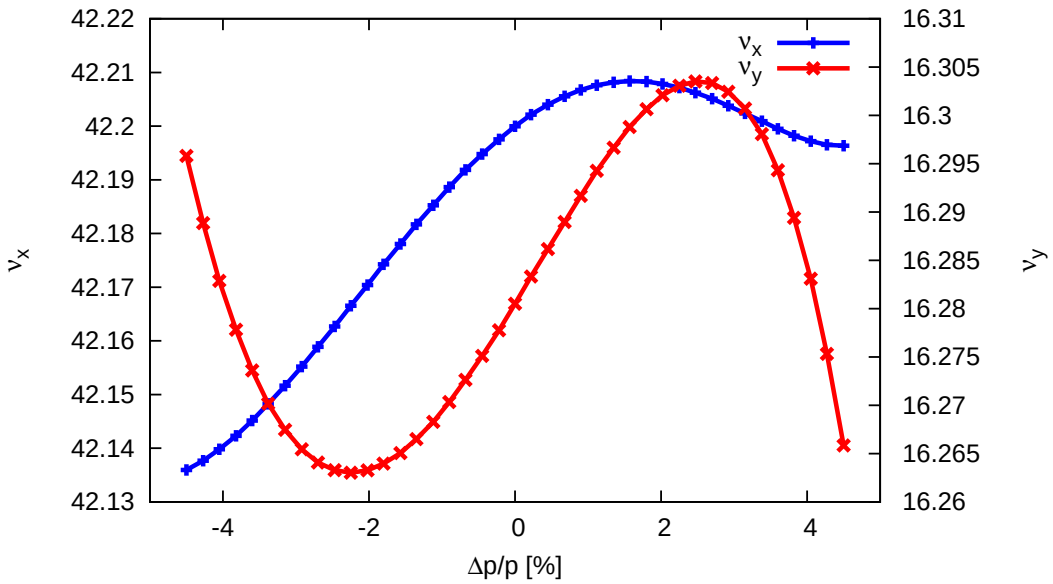

Figure 7: Chromaticity of a ring with ten IVUs calculated by Tracy-3 using the new sextupole settings of the 420 nonlinear optics branch. The range chosen corresponds to the required MA of the ring.

The on-momentum DA is almost unchanged which is a consequence of the almost identical ADTS between the two configurations. On-momentum FMA confirms the conclusions drawn from DA, but in addition, indicates crossing of the skew octupole resonance $2\nu_x + 2\nu_y = 117$ (this can be recognized as the semicircular band cutting through the frequency map at $2\,\text{mm} \leq y \leq 3\,\text{mm}$. This was not encountered in the bare lattice frequency map as the resonance line was not crossed in that configuration. This is the one significant difference of on-momentum ADTS between the two configurations. However, since the in-vacuum IDs limit the vertical acceptance of the machine, we note that the maximum vertical aperture available to the beam in the center of the long straight is around $y = \pm 2\,\text{mm}$, i.e. before the area of increased diffusion is reached.

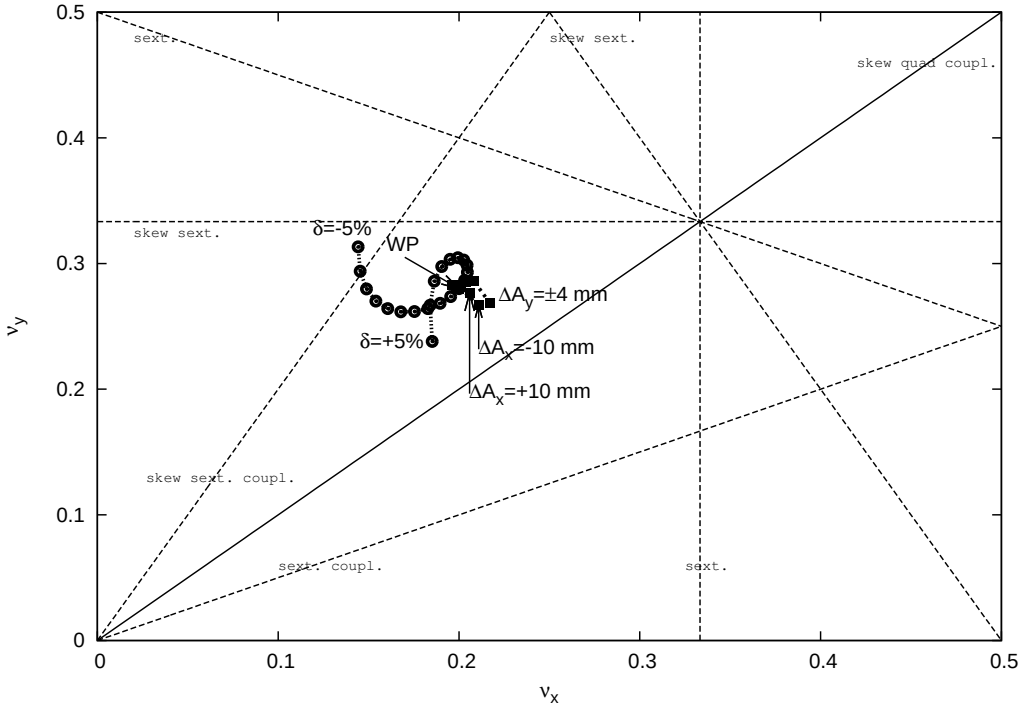

Figure 8: A plot of fractional tune space for the MAX IV 3 GeV storage ring with ten IVUs as calculated by OPA. Resonance and skew resonance lines have been included up to third order. WP indicates the working point. The step size chosen for the chromatic tune shift is 0.5% and 2.5 mm [1.0 mm] for the horizontal [vertical] amplitude-dependent tune shift.

For the off-momentum FMA we note that tune diffusion appears very similar between the two configuration. The notable exception is that in the loaded ring case the skew octupole resonance $2\nu_x + 2\nu_y = 117$ is only touched by the chromatic excursion at a single location rather than crossed twice (bare lattice case): the effect is that only a single band appears around $\delta = +1.25$ instead of two separate bands around $\delta = +2$. A significant effect on Touschek lifetime can however not be expected from this small difference. OPA estimates for dynamic Touschek lifetime indicate a 35% reduction of Touschek lifetime in the loaded ring case, however this is mainly explained by the reduced rf acceptance (at maximum cavity voltage $\delta_{\mathrm{rf}} = 7\% \rightarrow 6\%$ because of the extra radiation losses from the ten IVUs) and doesn't result from an actual decrease in the lattice MA.

We may conclude that, even in the presence of many strong IDs that require many local as well as a global linear optics matching, the nonlinear optics should be

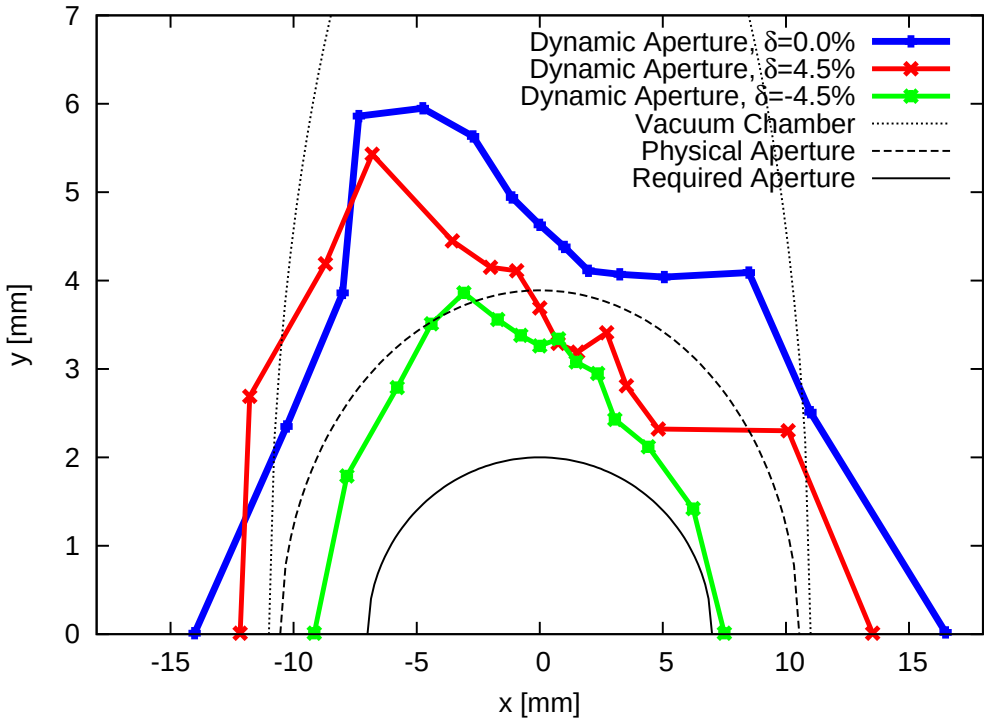

Figure 9: Dynamic aperture at the center of an unoccupied straight section in the MAX IV 3 GeV storage ring with ten IVUs. Tracking was performed with Tracy-3 in 6D for half a synchrotron period. Physical aperture and acceptance are also indicated in the plot.

able to remain constant without substantial negative impact on injection efficiency and/or lifetime.

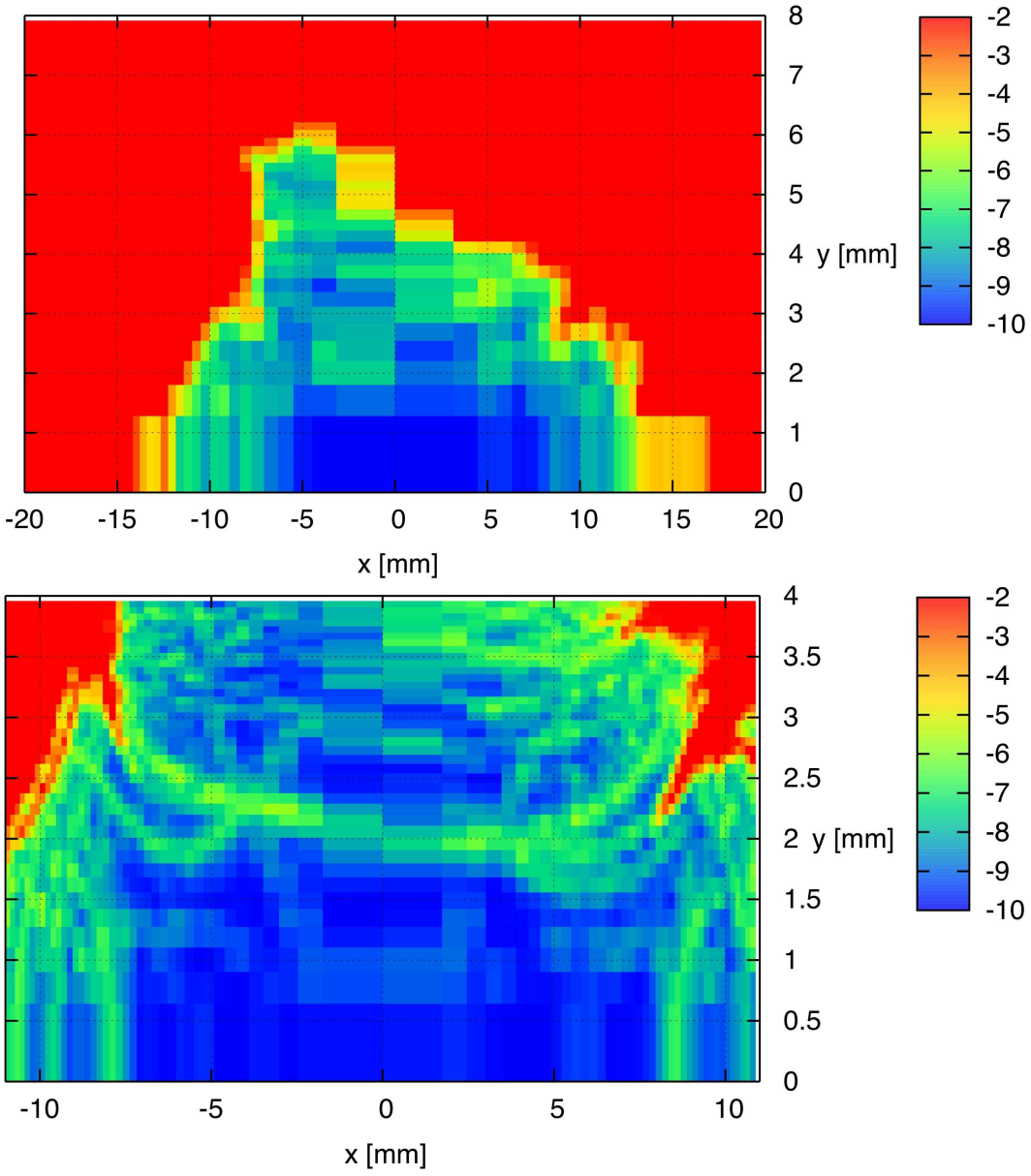

Figure 10: Diffusion maps for the MAX IV 3 GeV storage ring with ten IVUs taken at the center of an unoccupied straight section (physical acceptance at this location is $\pm 10.4\,\text{mm} \times \pm 3.9\,\text{mm}$). The lower plot is a magnification of the core area of the upper plot. Blue areas show small tune shifts, red areas show large tune shifts and particle loss. The plots have been generated with Tracy-3 by scanning transverse configuration space on-momentum and tracking for 2048 turns.

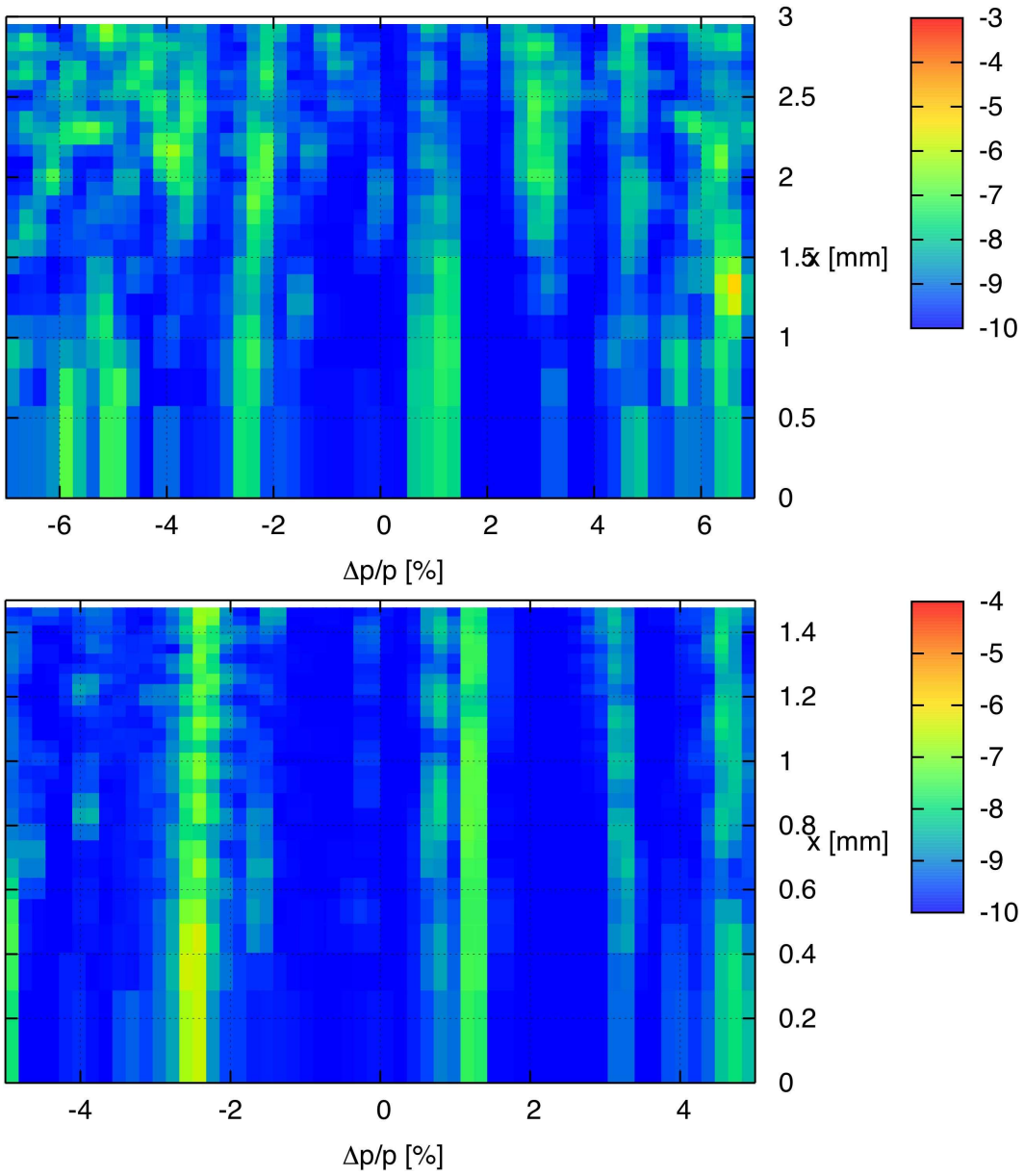

Figure 11: Diffusion maps for the MAX IV 3 GeV storage ring with ten IVUs taken at the center of an unoccupied straight section for off-momentum particles. The lower plot is a magnification of the core area of the upper plot. Blue areas show small tune shifts, red areas show large tune shifts and particle loss. The plots have been generated with Tracy-3 by scanning the horizontal coordinate and momenta and tracking for 2048 turns. The initial vertical amplitude was $+1$ mm.

6 Expected Performance of the New Lattice

This section attempts to give performance estimates for the new lattice in a realistic environment, e.g. a situation where the lattice is subjected to alignment errors, has magnets with field and multipole errors, and has been loaded with IDs with the expected imperfections. The first part deals with errors and their effect on dynamic aperture of the new lattice. The section after then summarizes emittance — both with and without the effect of intrabeam scattering (IBS) — and expected Touschek lifetime.

6.1 A Realistic Machine – the New Lattice with Errors

6.1.1 Bare Lattice

In this section errors are applies to the bare lattice as well as to a lattice with installed IDs. The IDs are modeled both with a simple ID approximation available in Tracy-3 and with kick maps as presented in the DDR. The error models used are almost exactly the same as in the DDR. An important difference is that the magnetic field errors were assumed to be Gaussian with 0.05% rms and a cut-off at 2σ as this is a better representation of the 20 μm peak-to-peak machining accuracy we expect from magnet manufacturing.

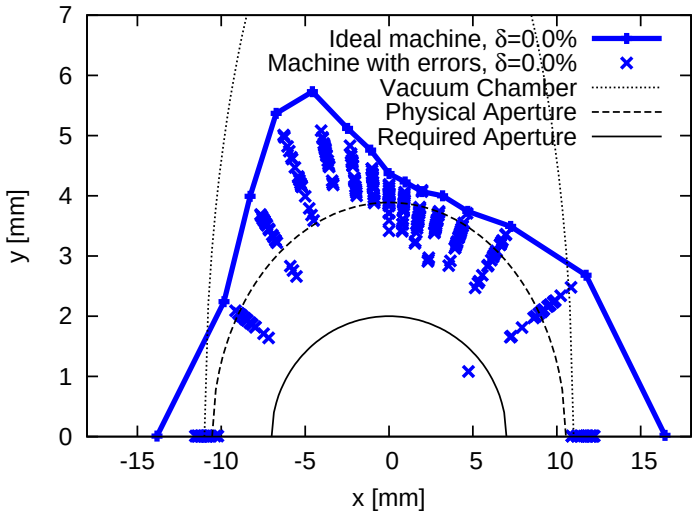

Figure 12: Dynamic aperture at the center of the long straight section in the MAX IV 3 GeV storage ring (bare lattice) from tracking with Tracy-3. The plots show the ideal lattice and results for 20 seeds with field and multipole errors.

A first example in Fig. 12 displays the effect of field and multipole errors for the new lattice in its bare configuration. Misalignments have not been added. The dynamic aperture has been calculated with Tracy-3 for on-energy particles for one synchrotron period. Along with the ideal machine DA, the results for 20 seeds are given.

This can be compared to the situation where only misalignment errors have been applied (displayed in Fig. 13). The misalignment errors correspond to the "required" model of the DDR that has been modified in two ways:

- BPM misalignment errors were reduced to 3 μm rms calibration accuracy.
- Magnet block misalignments were reduced to 50 μm rms. Survey and alignment experts expect less than 100 μm displacement of neighboring blocks. This is modeled as Gaussian distribution with a 2σ cut-off.

Note that the reduction of DA here is more significant than in the case with only field and multipole errors.

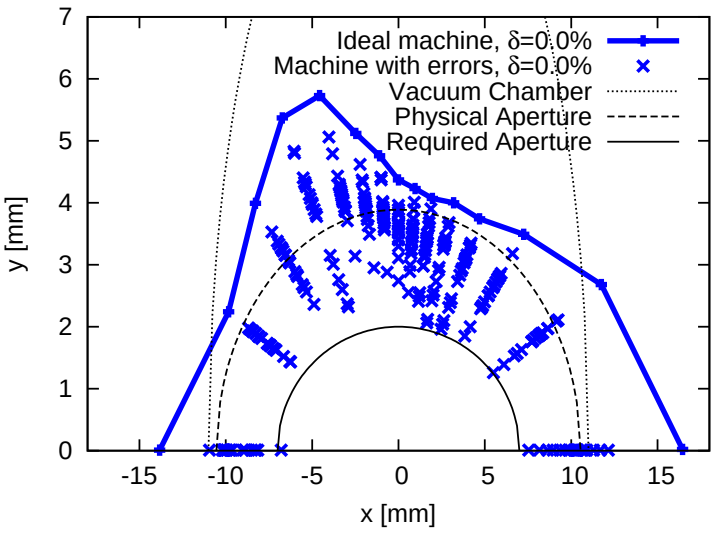

Figure 13: Dynamic aperture at the center of the long straight section in the MAX IV 3 GeV storage ring (bare lattice) from tracking with Tracy-3. The plot shows the ideal lattice and results for 20 seeds with misalignments.

Finally, Fig. 14 shows the result for DA of the bare lattice with the effects of all error sources: field and multipole errors as well as misalignments. This figure indicates that misalignment errors dominate the resulting DA at the currently assumed

level of field and multipole errors. As a consequence there is only little a difference between the DA of a machine that has been misaligned only (Fig. 13) and a machine where all errors have been applied (Fig. 14). It must also be noted that while the DA reduction from errors is significant, for most seeds the resulting DA still extends beyond the required aperture and therefore should not significantly reduce Touschek lifetime or injection efficiency.

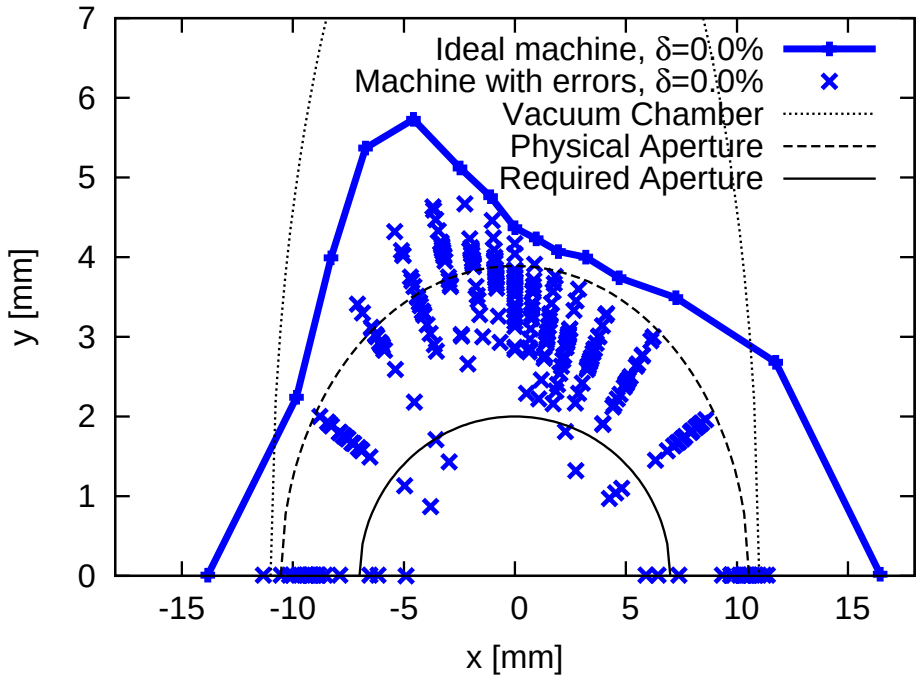

Figure 14: Dynamic aperture at the center of the long straight section in the MAX IV 3 GeV storage ring (bare lattice) from tracking with Tracy-3. The plot shows the ideal lattice and results for 20 seeds with field and multipole errors as well as misalignments.

In terms of alignment targets, it is interesting to compare the presently anticipated situation (Fig. 14) to the situation depicted in Fig. 15. Here, the alignment errors have been reduced to 25 μm rms with a roll error of 0.1 mrad rms. Otherwise no changes have been made to the error models. Note that this situation shows more than adequate DA everywhere and for all seeds (apart from a single outlier). The alignment errors still dominate the overall DA, but the DA reduction caused by alignment errors is now closer to that resulting from field and multipole errors — an overall more balanced situation. It can therefore be contemplated if this misalignment model should serve as a target (albeit a challenging one) for survey and alignment procedures.

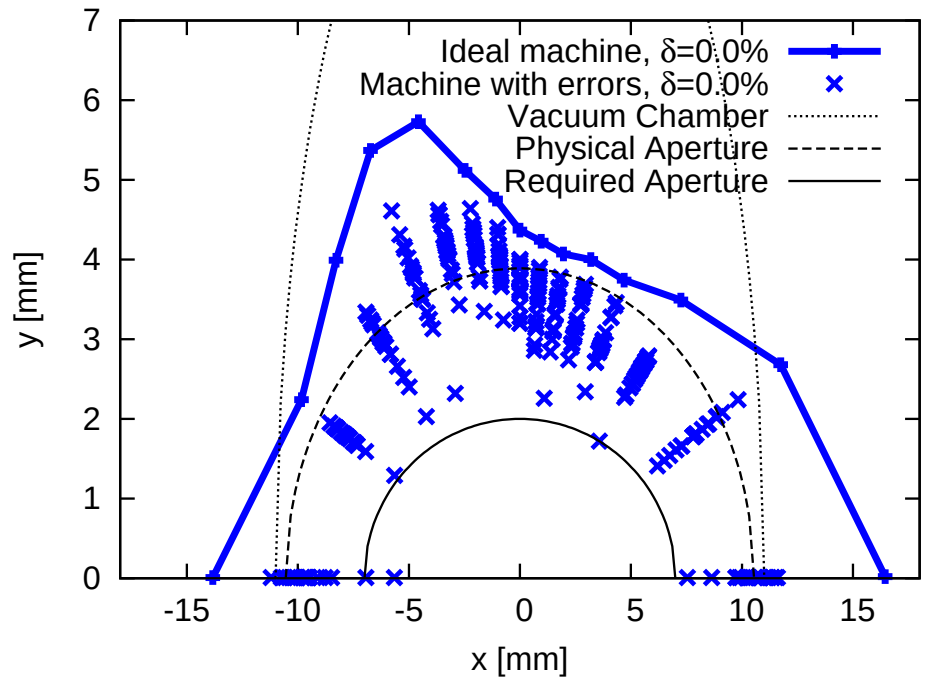

Figure 15: Dynamic aperture at the center of the long straight section in the MAX IV 3 GeV storage ring (bare lattice) from tracking with Tracy-3. The plot shows the ideal lattice and results for 20 seeds with field and multipole errors as well as misalignments. The girder misalignments here have however been reduced to 25 μm rms with a roll error of 0.1 mrad rms.

6.1.2 Lattice with IDs

The effect of errors on a machine with IDs of course also has to be investigated. For this purpose we add ten in-vacuum undulators of type pmuL (cf. Table 2) as this is a realistic scenario for standard operation of the MAX IV 3 GeV storage ring after commissioning has been completed and regular user operation is under way. These IDs can be added to the bare lattice in two ways: the first method uses the built-in wiggler model in Tracy-3 while the second method makes use of kick maps generated with RADIA [5] that can be included when tracking with Tracy-3.

In principle the kick map method is of advantage since it contains all relevant effects of the ID on the stored beam including potentially harmful properties such as field roll-off. There is however one substantial disadvantage to tracking with kick maps. Kick maps are only defined up to a certain boundary (for the kick maps used

here it is $\pm$ 20 mm in x and $\pm$ 2 mm in y). During tracking, if a particle reaches such a boundary it is considered lost. Therefore, tracking with kick maps means that acceptance is always introduced in DA calculations. But usually, DA calculations are performed without actual physical apertures present in order to display purely dynamic effects of the magnet lattice rather than also including acceptance limitations form physical apertures. If kick map results for DA are displayed, the actual DA is masked by the acceptance of the kick map. Since the DA is rather large in the MAX IV 3 GeV storage ring (i.e. comparable or larger than the physical aperture), this masking is significant.

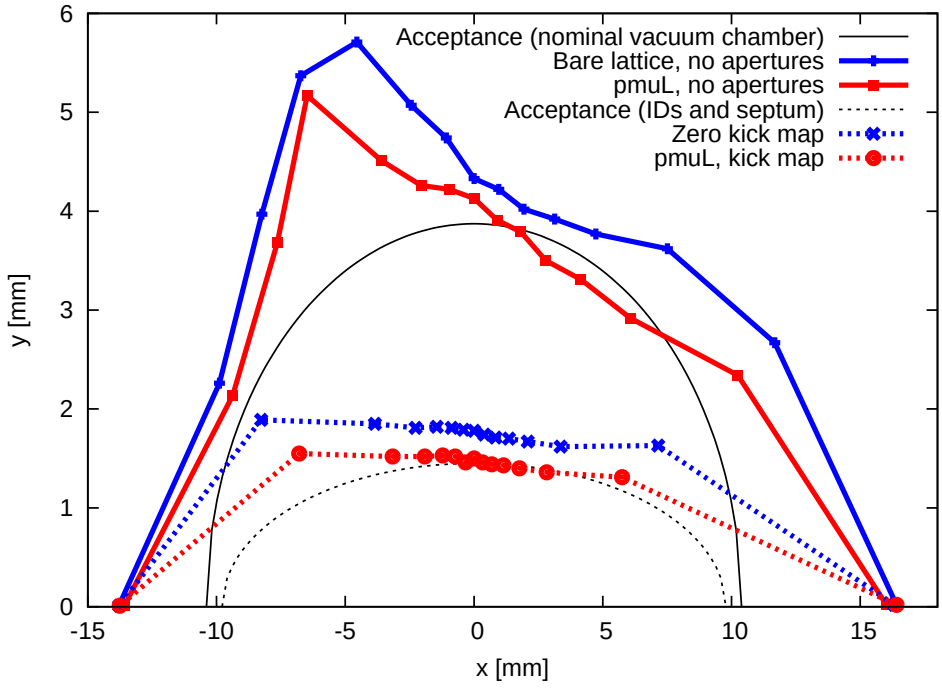

Figure 16: Dynamic aperture at the center of the long straight section in the MAX IV 3 GeV storage ring (bare lattice). Tracking was performed with Tracy-3 in 6D for half a synchrotron period (particles initially on energy, i.e. $\delta = 0\%$). The plot compares pure DA (solid red and blue lines) with DA masked by the acceptance introduced by finite kick map boundaries (dashed red and blue lines).

An example for this issue is given in Fig. 16. In this study 6D tracking with Tracy-3 for half a synchrotron period with a bare lattice is compared to the same tracking for a lattice with a single pmuL installed . For the case with pmuL installed tracking has been carried out once using the built-in ID model and once using the

kick map. This is compared to the bare lattice case that has been carried out using the bare lattice and a bare lattice with a "zero kick map" (a kick map identical to the one used for pmuL, but with zero kicks inserted at all positions) installed in the long straights. What this comparison shows is that both the ID model and the kick map predict a DA reduction compared to the bare lattice of comparable amount. However, the severely reduced DA for the pmuL kick map case is shown to be the result of acceptance masking DA as the zero kick map (which has no dynamic effect on the beam) shows roughly the same reduction. We can therefore conclude, that the purely dynamic reduction caused by pmuL is revealed in tracking using both methods. However, the overall DA reduction observed when using kick maps is caused mainly by the limited acceptance and not detrimental effect of pmuL itself. Therefore, in the following study the ID model is used for tracking rather than the kick maps. This allows an inspection of the actual *dynamic* aperture without any masking by acceptance.

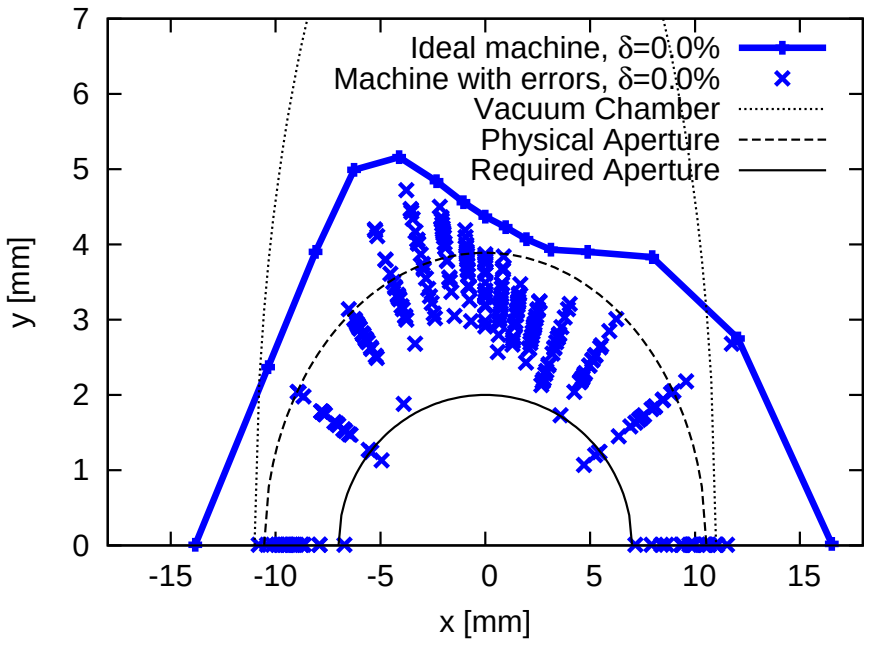

Figure 17: Dynamic aperture at the center of the long straight section in the MAX IV 3 GeV storage ring from tracking with Tracy-3. In addition to the bare lattice, ten pmuL have been added to the ring. The plot shows the ideal lattice and results for 20 seeds with field and multipole errors as well as misalignments.

Figure 17 shows Tracy-3 results from tracking a lattice with ten pmuL installed

and matched. The DA is displayed for the ideal machine and for 20 seeds with field, multipole, and alignment errors. The ideal DA differs from that of the bare lattice (cf. Fig. 14) as a result of the installed IDs. The error seeds however, show a dense consistent pattern. Most importantly, while the DA reduction from errors is not negligible, the resulting DA for a majority of all seeds extends beyond the required aperture and therefore should not significantly reduce Touschek lifetime or injection efficiency. This is a very encouraging result. There remains the issue of dynamic skew quadrupole and multipole errors from closed ID gaps. This is not revealed by the ID model or the kick maps and it is not included in the multipole error model. Acceptable limits for such errors contributions have been calculated [4]. Once actual IDs have been manufactured and their dynamic multipole errors (after local correction with e.g. skew quadrupoles and current strips) have been measured, such errors can be added to the model and tracking results generated. For the moment it suffices to conclude that as long as ID multipolar contributions are within specified limits, no unacceptably large blow-up of vertical emittance or reduction of lifetime and injection efficiency should be expected.

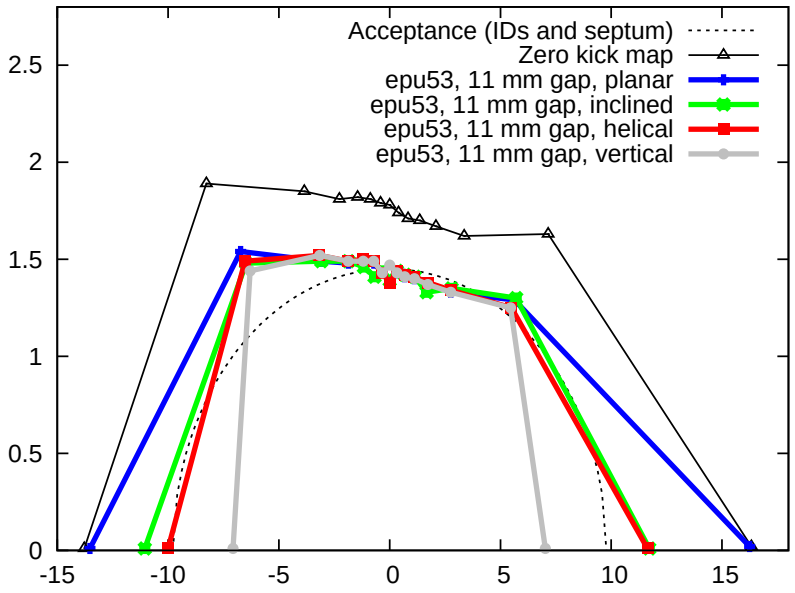

Figure 18: Dynamic aperture at the center of the long straight section in the MAX IV 3 GeV storage ring. A single epu53 has been added to the bare lattice. Tracking was performed with Tracy-3 in 6D for half a synchrotron period (particles initially on energy, i.e. $\delta = 0\%$).

Finally, we note that there are nevertheless good reasons to investigate DA with

kick maps. An example is displayed in Fig. 18 which has been taken from [4]. Only the kick maps allow proper modeling of the different modes of an elliptically polarizing undulator (EPU). With the kick maps the different levels of DA reduction corresponding to the chosen EPU mode can be quantified. In Fig. 18 epu53 (undulator parameters given in [4]) is modeled with kick maps for different polarizations and the resulting DA shows that while all modes give roughly the same vertical DA (which is as expected heavily dominated by the vertical acceptance of the kick map), the horizontal DA is lowest for the vertical mode and highest for the planar mode with the inclined and helical modes in between. This level of detail requires use of kick maps.

It is however important to note again that the vertical DA reduction is primarily a consequence of the kick map acceptance and not caused by imperfections of the ID. And specifically, the kick map for epu53 introduces an entirely artificial acceptance limitation. Since epu53 is operated at gaps as low as 11 mm, the available aperture in epu53 will be on the order of ± 4 mm, the kick map however artificially limits the aperture to ± 2 mm (cf. zero kick map in Fig. 18).

6.2 Emittance, Intrabeam Scattering, Touschek Lifetime

The ultralow emittance of the MAX IV 3 GeV storage ring has two interesting consequences:

- The equilibrium emittance is determined by the lattice and the ID gap settings.
- The equilibrium emittance is determined by both lattice emittance and intrabeam scattering (IBS).

Since IBS depends heavily on the charge density in 6D phase space, the applied cavity voltage and bunch lengthening from Landau cavities (LCs) governs the resulting emittance. Since Touschek lifetime also depends strongly on charge density in 6D phase space it varies as a function of overall emittance including IBS as well as bunch lengthening. Because of this nontrivial interplay between several factors in the realistic machine, the plan here will be to investigate several "base line" configurations of the MAX IV 3 GeV storage ring and then show consequences for variation of specific parameters like main cavity voltage or bunch lengthening achieved with the LCs. All calculations shall be carried out assuming 500 mA stored beam current in all buckets with no ion-clearing gap (i.e. 5 nC charge per bunch).

The MAX IV 3 GeV storage ring has six main rf cavities for a maximum overall accelerating voltage of 1.8 MV. The ring also has three third-harmonic LCs that should allow bunch lengthening by up to 68 mm rms (more than a factor 5!) ac-

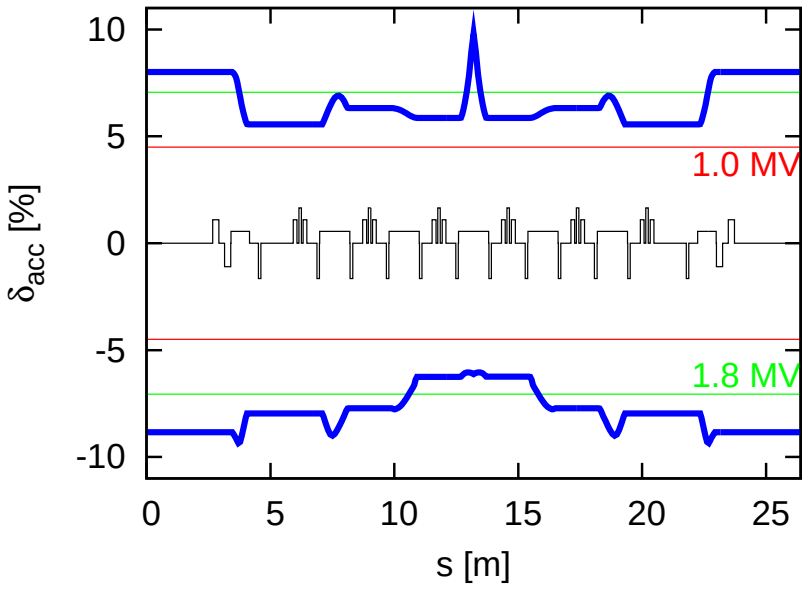

Figure 19: Momentum acceptance for one achromat of the MAX IV 3 GeV storage ring. A bare lattice (11 mm chamber apertures) and cavities at maximum voltage 1.8 MV have been assumed (green line, corresponds to 7% MA). For comparison, the red line shows 1.02 MV which corresponds to 4.5% MA in this configuration. Momentum acceptance tracking was performed with OPA for half a synchrotron period. The blue line shows overall MA.

cording to the DDR [3]. Originally the lattice was designed to give a momentum acceptance (MA) of 4.5%. Studies performed with the new lattice version show however, that the lattice can deliver significantly more MA if sufficient rf overvoltage is available. Such a situation is displayed in Fig. 19 where the MA for one achromat of the bare lattice (using standard 11 mm aperture chambers throughout the entire achromat, i.e. a first approximation) is given assuming the rf cavities are driven at the maximum voltage of 1.8 MV corresponding to an rf acceptance of 7% (green line). The lattice acceptance is indeed substantially higher than the 4.5% design so that the resulting overall MA (blue line) is also higher. This holds as long as sufficient rf voltage is available. If the rf voltage is reduced sufficiently it will start to determine the overall MA. This situation is also shown in the figure: if 1.02 MV overall cavity voltage (red line) is applied, the rf acceptance is reduced to 4.5%. One consequence of such a situation is that Touschek lifetime calculations in 6D (which are derived from tracking and thus require a lot of CPU time) can be approximated

well by a linear simplification (available in both Tracy-3 and OPA) [6].

Table 10 shows results for emittance, IBS, and Touschek lifetime for the MAX IV 3 GeV storage ring bare lattice in different configurations. The first cases show a situation where the coupling is adjusted to 2.5% setting the vertical emittance at the 1 Å diffraction limit. At first no LCs are used to stretch the bunches. When IBS is included the emittance increases as one would expect. The coupling then needs to be adjusted to 1.7% to get back to the required vertical beam size.

Table 10: Overview of emittances, IBS, and Touschek lifetime for different configurations of the bare lattice. Without IBS the natural emittance for this lattice is $\varepsilon_0 = 326\,\text{nm rad}$ and the synchrotron radiation losses are 360 keV/turn. The total rf voltage has been set to $U_{\text{cav}} = 1.8\,\text{MV}$ which corresponds to of $\delta_{\text{rf}} = 7.06\%$. The star ($\star$) indicates IBS included. Touschek lifetime figures in parentheses indicates results from linear approximation.

IBS	κ	ε_y [pm rad]	ε_x [nm rad]	σ_s [mm]	$\sigma_\delta \times 10^{-3}$	τ_{ts} [h]
1 Å diffraction limit, no LCs						
	2.5%	8.0	0.318	8.81	0.768	19.1 (41.1)
$\star$	2.5%	11.6	0.460	11.12	0.9692	(55.1)
$\star$	1.7%	8.0	0.464	11.12	0.9692	22.7 (45.6)
1 Å diffraction limit, LCs tuned in						
	2.5%	8.0	0.318	50.0	0.768	108.1 (233.5)
$\star$	2.5%	9.1	0.361	54.27	0.8336	(256.8)
$\star$	2.2%	**8.0**	**0.362**	54.27	0.8336	**114.3 (240.6)**
High-brightness mode, no LCs						
	0.6%	2.0	0.324	8.81	0.768	9.4 (20.3)
$\star$	0.6%	3.4	0.549	12.28	1.070	(31.6)
$\star$	0.4%	2.0	0.550	12.28	1.070	12.4 (24.2)
High-brightness mode, LCs tuned in						
	0.6%	2.0	0.324	50.0	0.768	53.6 (115.4)
$\star$	0.6%	2.5	0.403	57.62	0.8851	(136.9)
$\star$	0.5%	**2.0**	**0.403**	57.62	0.8851	**59.5 (122.7)**

For comparison, the LCs are tuned in to stretch the bunches to 50 mm. If IBS is included this elongates the bunches a bit more, but the overall length is still well within the capabilities of the 3rd harmonic rf system. Finally, the coupling is again

adjusted to get the desired vertical beam size.

Overall, IBS blows up the horizontal emittance by 46% without LCs but by only 14% when the LCs are tuned in. Since the LCs reduce the effect of IBS, the blow-up of bunch length and energy spread are also much less severe when operating with LCs tuned in. The Touschek lifetime (including IBS) is 23 h without LCs but 114 h with LCs. This latter figure is certainly more than sufficient and would actually lead to a situation where the overall lifetime is actually no longer Touschek-dominated at all. This is rather unusual for a modern third-generation light source.

In the second case a so-called "high-brightness mode" is investigated where the coupling is chosen so the vertical emittance is 2 pm rad. The procedure detailed above was followed also here. The emittance blowup caused by IBS is more severe because of the increased charge density as a consequence of the vertical squeeze. The horizontal emittance blowup is now 70% without LCs but only 24% when the LCs are tuned in. Touschek lifetime (including IBS) is 12 h without LCs and 60 h with LCs which is again sufficient.

As can be inferred from Fig. 19, operating the bare lattice with maximum cavity voltage is not necessarily required to to achieve sufficient Touschek lifetime. Therefore, a second bare lattice configuration is investigated in Table 11 where the cavity voltage has been reduced so that the original design rf acceptance of $\delta_{\mathrm{rf}} = 4.5\%$ is achieved. Since rf power is directly connected to running costs of the facility, it is of interest to investigate the performance impact of running at reduced cavity voltage in a configuration where radiation losses are low. Since the rf acceptance is now lower than the lattice acceptance throughout the entire machine, the Touschek lifetime calculated with 6D tracking in Tracy-3 is identical to the linear approximation from OPA.

As one would expect, the natural bunch length is increased by the reduced rf acceptance. In the 1 Å diffraction limit a horizontal emittance blowup of 38% (without LCs) and 14% (with LCs) is recognized. So if the LCs are tuned in, this blowup is identical to the case where a high rf acceptance (1.8 MV cavity voltage) is set. Touschek lifetime is increased from 9 h to 32 h by the LCs. In the high-brightness case Touschek lifetime without the LCs is 4 h which is rather low (even with top-up operation, losses should be kept as low as possible in the interest of radiation protection), however, with LCs tuned in this increases to 17 h which should be sufficient. As originally stipulated, with the bare lattice (and LCs tuned in), the overall cavity voltage can be reduced without reducing Touschek lifetime to unacceptable levels.

Table 11: Overview of emittances, IBS, and Touschek lifetime for different configurations of the bare lattice. Without IBS the natural emittance for this lattice is $\varepsilon_0 = 326\,\mathrm{nm\,rad}$ and the synchrotron radiation losses are 360 keV/turn. The total rf voltage has been set to $U_{\mathrm{cav}} = 1.02\,\mathrm{MV}$ which corresponds to of $\delta_{\mathrm{rf}} = 4.5\%$. The star ($\star$) indicates IBS included. Touschek lifetime figures in parentheses indicates results from linear approximation.

IBS	κ	ε_y [pm rad]	ε_x [nm rad]	σ_s [mm]	$\sigma_\delta \times 10^{-3}$	τ_{ts} [h]
1 Å diffraction limit, no LCs						
	2.5%	8.0	0.318	12.0	0.768	7.1 (7.2)
$\star$	2.5%	11.0	0.436	14.65	0.9375	(10.3)
$\star$	1.8%	8.0	0.439	14.65	0.9375	8.7 (8.8)
1 Å diffraction limit, LCs tuned in						
	2.5%	8.0	0.318	50.0	0.768	29.7 (30.0)
$\star$	2.5%	9.1	0.361	54.27	0.8336	(34.6)
$\star$	2.2%	**8.0**	**0.362**	54.27	0.8336	**32.2 (32.4)**
High-brightness mode, no LCs						
	0.6%	2.0	0.324	12.0	0.768	3.5 (3.6)
$\star$	0.6%	3.2	0.514	16.08	1.029	(6.1)
$\star$	0.4%	2.0	0.515	16.08	1.029	4.8 (4.9)
High-brightness mode, LCs tuned in						
	0.6%	2.0	0.324	50.0	0.768	14.8 (14.9)
$\star$	0.6%	2.5	0.403	57.62	0.8851	(19.2)
$\star$	0.5%	**2.0**	**0.403**	57.62	0.8851	**17.0 (17.2)**

Figure 20 attempts to summarize the bare lattice Touschek lifetime as a function of cavity voltage, i.e. rf acceptance. In the figure the bare lattice has been assumed with 500 mA stored current. The effect of IBS was included, no LCs were assumed, i.e. the natural bunch lengths with only IBS lengthening was applied. Emittance coupling was adjusted so the vertical emittance was held constant at $\varepsilon_y = 8\,\mathrm{pm\,rad}$. At a cavity voltage of around 1.3 MV the linearized approximation for Touschek lifetime starts to deviate from the actual 6D tracking result. It is here ($\delta_{\mathrm{rf}} \simeq 5.6\%$) where the lattice MA starts clipping the rf acceptance. For the cases displayed here the LCs can stretch the bunches by a factor 2–5 which increases Touschek lifetime accordingly. For the "high-brightness mode", the lifetime is roughly 50% of the

lifetime shown here.

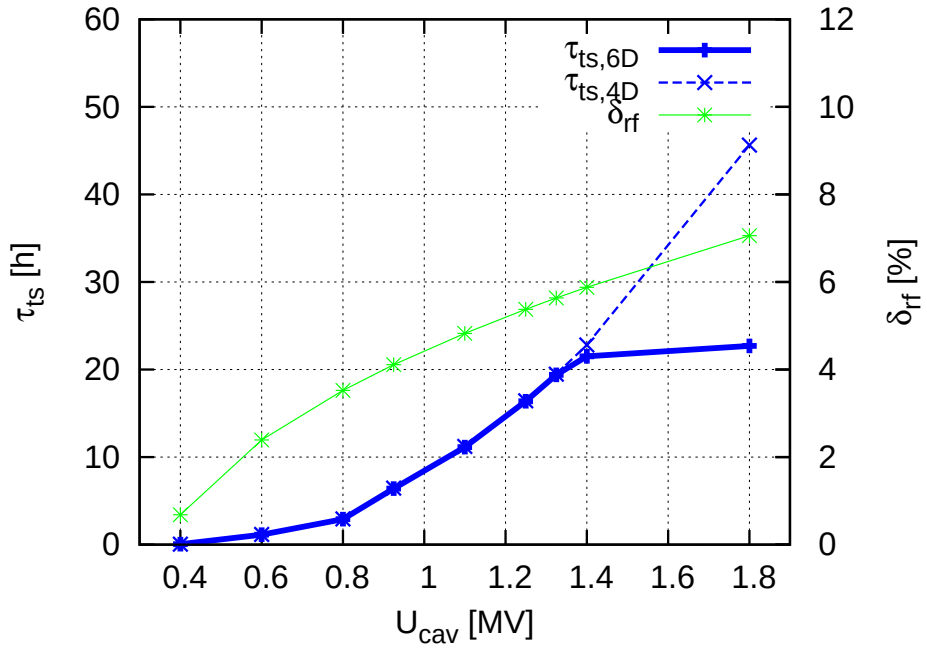

Figure 20: Touschek lifetime (blue) and rf acceptance (green) of the MAX IV 3 GeV storage ring bare lattice for different cavity voltages. 11 mm chamber apertures and 500 mA stored current were assumed. The effect of IBS was included with coupling adjusted to give $\varepsilon_y =$ 8 pm rad. No LCs were included.

The next scenario demonstrates a lattice with a single pmuL installed and overall cavity voltage again set to 1.8 MV. The purpose of this scenario is mainly to show the effect of a strong ID on the otherwise bare lattice. The pmuL adds an extra 23 keV/turn to the radiation losses. The equilibrium emittance is reduced by 12 pm rad. Results from tracking for this scenario are displayed in Table 12.

The situation is fairly similar to the bare lattice case except that because of the added radiation damping from the pmuL, the IBS emittance blowup is reduced and consequently lifetime is a bit lower. Horizontal emittance blowup is 47% without LCs and 14% with LCs. The Touschek lifetime is increased by the LCs by a little more than a factor five. For the high-brightness case the horizontal emittance blowup is obviously more severe: 72% without LCs and 25% with LCs. In both cases the Touschek lifetime is however more than sufficient and a reduction of overall cavity voltage could again be considered.

Table 12: Overview of emittances, IBS, and Touschek lifetime for different configurations of the lattice where a single pmuL has been added. Without IBS the natural emittance for this lattice is $\varepsilon_0 = 314\,\text{nm rad}$ (the pmuL has reduced the emittance by 12 pm rad) and the synchrotron radiation losses are 386 keV/turn (the pmuL has added 26 keV per turn). The total rf voltage has been set to $U_{\text{cav}} = 1.8\,\text{MV}$ which corresponds to of $\delta_{\text{rf}} = 6.961\%$. The star ($\star$) indicates IBS included. Touschek lifetime figures in parentheses indicates results from linear approximation.

IBS	κ	ε_y [pm rad]	ε_x [nm rad]	σ_s [mm]	$\sigma_\delta \times 10^{-3}$	τ_{ts} [h]
1 Å diffraction limit, no LCs						
	2.6%	8.0	0.306	8.85	0.770	19.4 (39.5)
$\star$	2.6%	11.7	0.447	10.98	0.9550	(51.6)
$\star$	1.8%	8.0	0.451	10.98	0.9550	22.3 (42.6)
1 Å diffraction limit, LCs tuned in						
	2.6%	8.0	0.306	50.0	0.770	109.3 (223.4)
$\star$	2.6%	9.1	0.348	53.88	0.8298	(257.0)
$\star$	2.3%	**8.0**	**0.349**	53.88	0.8298	**121.6 (240.4)**
High-brightness mode, no LCs						
	0.6%	2.0	0.312	8.85	0.770	9.6 (19.5)
$\star$	0.6%	3.4	0.536	12.07	1.050	(29.4)
$\star$	0.4%	2.0	0.537	12.07	1.050	12.1 (22.4)
High-brightness mode, LCs tuned in						
	0.6%	2.0	0.312	50.0	0.770	54.2 (110.3)
$\star$	0.6%	2.5	0.390	56.97	0.8773	(128.9)
$\star$	0.6%	**2.0**	**0.391**	56.97	0.8773	**58.9 (115.2)**

A case that most closely resembles actual operating conditions during user operation is summarized in Table 13. In this case ten pmuL are added to an otherwise bare lattice. The IDs reduce the equilibrium emittance by 80 pm rad and increase the losses by 261 keV/turn. The cavities are set to maximum voltage which then gives an rf acceptance of just over 6%.

In the 1 Å diffraction limit case, IBS blows up the horizontal emittance by 57% without LCs and 17% with LCs. Touschek lifetime is still sufficiently high despite increased losses (which reduces overvoltage). Note also that with everything else

held constant, emittance reduction equates to *increased* lifetime [7]. Even without LCs 21 h are achieved, while 114 h can be expected with the LCs tuned in properly.

In the high-brightness mode the emittance blowup is again more severe: 88% without LCs while 30% are noted if LCs are tuned in. Touschek lifetime is 10 h without LCs and 56 h with LCs which is more than sufficient. So even when a large number of IDs is added to the storage ring, the overall cavity voltage does not need to be operated near maximum to achieve good lifetime. There is ample margin left for more IDs. This shall be investigated next.

Table 13: Overview of emittances, IBS, and Touschek lifetime for different configurations of the lattice where ten pmuL have been added. Without IBS the natural emittance for this lattice is $\varepsilon_0 = 234\,\text{nm rad}$ (the ten pmuL have reduced the emittance by 80 pm rad) and the synchrotron radiation losses are 621 keV/turn (the ten pmuL have added 261 keV per turn). The total rf voltage has been set to $U_{\text{cav}} = 1.8\,\text{MV}$ which corresponds to of $\delta_{\text{rf}} = 6.05\%$. The star ($\star$) indicates IBS included. Touschek lifetime figures in parentheses indicates results from linear approximation.

IBS	κ	ε_y [pm rad]	ε_x [nm rad]	σ_s [mm]	$\sigma_\delta \times 10^{-3}$	τ_{ts} [h]
1 Å diffraction limit, no LCs						
	3.5%	8.0	0.226	9.14	0.779	21.5 (24.9)
$\star$	3.5%	12.4	0.350	10.45	0.8910	(29.2)
$\star$	2.3%	8.0	0.354	10.45	0.8910	20.5 (23.3)
1 Å diffraction limit, LCs tuned in						
	3.5%	8.0	0.226	50.0	0.779	117.5 (136.3)
$\star$	3.5%	9.3	0.263	52.27	0.8144	(142.4)
$\star$	3.0%	**8.0**	**0.264**	52.27	0.8144	**114.3 (131.6)**
High-brightness mode, no LCs						
	0.9%	2.0	0.232	9.14	0.779	10.6 (12.3)
$\star$	0.9%	3.7	0.434	11.19	0.9537	(16.1)
$\star$	0.5%	2.0	0.436	11.19	0.9537	10.4 (11.7)
High-brightness mode, LCs tuned in						
	0.6%	2.0	0.232	50.0	0.779	57.8 (67.0)
$\star$	0.9%	2.6	0.301	54.16	0.8438	(73.3)
$\star$	0.7%	**2.0**	**0.302**	54.16	0.8438	**56.1 (64.2)**

Figure 21 attempts to summarize the bare lattice Touschek lifetime as a function of cavity voltage, i.e. rf acceptance. In the figure the lattice with ten pmuL installed has been assumed with 500 mA stored current. The effect of IBS was included, no LCs were assumed, i.e. the natural bunch lengths with only IBS lengthening was applied. Emittance coupling was adjusted so the vertical emittance was held constant at $\varepsilon_y = 8\,\mathrm{pm\,rad}$. At a cavity voltage of around 1.7 MV the linearized approximation for Touschek lifetime starts to deviate from the actual 6D tracking result. It is here ($\delta_{\mathrm{rf}} \simeq 5.7\%$) where the lattice MA starts clipping the rf acceptance. For the cases displayed here the LCs can stretch the bunches by a factor 3–5 which increases Touschek lifetime accordingly. For the "high-brightness mode", the lifetime is roughly 50% of the lifetime shown here.

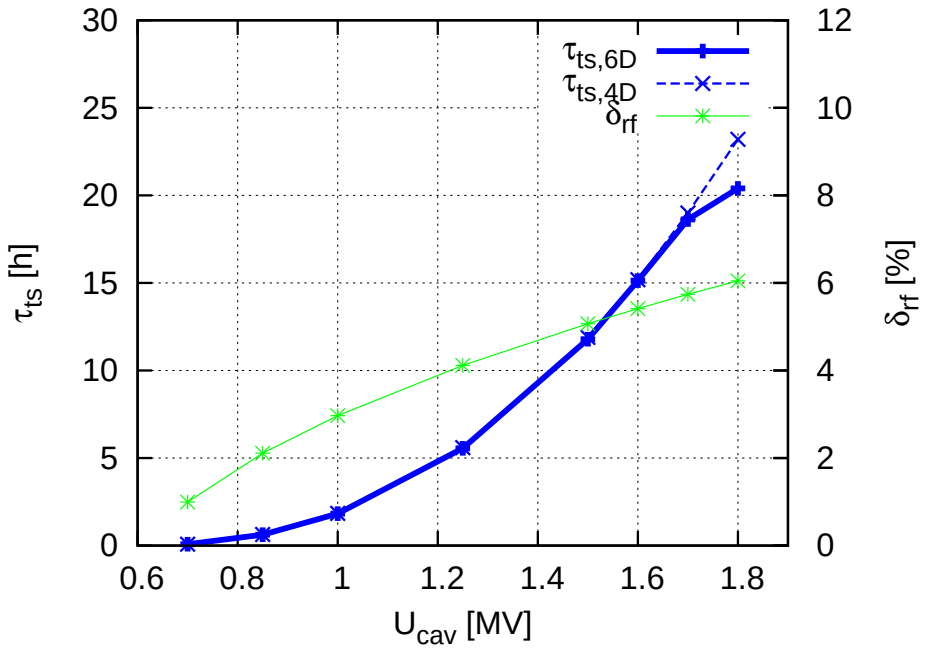

Figure 21: Touschek lifetime (blue) and rf acceptance (green) of the MAX IV 3 GeV storage ring with ten pmuL for different cavity voltages. 11 mm chamber apertures and 500 mA stored current were assumed. The effect of IBS was included with coupling adjusted to give $\varepsilon_y = 8\,\mathrm{pm\,rad}$. No LCs were included.

Table 14 shows results for a "fully loaded ring": 19 pmuL are installed so that every available user straight contains one such ID. The IDs reduce the equilibrium emittance by 139 pm rad so that without IBS an equilibrium emittance of 187 pm rad

is achieved. The IDs also increase the losses by 496 keV/turn. With total losses at 856 keV/turn and the cavities set to maximum voltage, an rf acceptance of 5.1% is achieved. Because of the large radiation losses (and despite running the cavities at maximum voltage), the overall MA is now determined mainly by the rf acceptance (cf. Fig. 19). Therefore, the Touschek lifetime derived from the simple approximation closely matches the actual Touschek lifetime derived from tracking.

Table 14: Overview of emittances, IBS, and Touschek lifetime for different configurations of the lattice where 19 pmuL have been added ("fully loaded ring"). Without IBS the natural emittance for this lattice is $\varepsilon_0 = 187$ nm rad (the 19 pmuL have reduced the emittance by 139 pm rad) and the synchrotron radiation losses are 856 keV/turn (the 19 pmuL have added 496 keV per turn). The total rf voltage has been set to $U_{\mathrm{cav}} = 1.8$ MV which corresponds to of $\delta_{\mathrm{rf}} = 5.102\%$. The star ($\star$) indicates IBS included. Touschek lifetime figures in parentheses indicates results from linear approximation.

IBS	κ	ε_y [pm rad]	ε_x [nm rad]	σ_s [mm]	$\sigma_\delta \times 10^{-3}$	τ_{ts} [h]
1 Å diffraction limit, no LCs						
	4.5%	8.0	0.179	9.48	0.782	13.0 (13.1)
$\star$	4.5%	12.8	0.287	10.48	0.8646	(15.0)
$\star$	2.7%	8.0	0.292	10.48	0.8646	11.7 (11.8)
1 Å diffraction limit, LCs tuned in						
	4.5%	8.0	0.179	50.0	0.782	68.5 (69.1)
$\star$	4.5%	9.5	0.212	51.69	0.8084	(71.6)
$\star$	3.7%	**8.0**	**0.213**	51.69	0.8084	**65.0 (65.6)**
High-brightness mode, no LCs						
	1.1%	2.0	0.185	9.48	0.782	6.4 (6.4)
$\star$	1.1%	3.9	0.363	11.07	0.9128	(8.2)
$\star$	0.5%	2.0	0.365	11.07	0.9128	5.8 (5.8)
High-brightness mode, LCs tuned in						
	1.1%	2.0	0.185	50.0	0.782	33.6 (33.9)
$\star$	1.1%	2.6	0.246	53.11	0.8306	(36.6)
$\star$	0.8%	**2.0**	**0.247**	53.11	0.8306	**31.4 (31.7)**

For the 1 Å diffraction limit case, IBS blows up the emittance by 63% without LCs and 19% with LCs. With the LCs the horizontal emittance including IBS can be

pushed to 0.21 nm rad. Touschek lifetime is still high despite reduced MA: without LCs 12 h are achieved, while 65 h can be expected with the LCs tuned in properly.

In the high-brightness mode the emittance blowup is again more severe: emittance more than doubles without LCs (+97%) while 34% are noted even with LCs tuned in. Touschek lifetime is 6 h without LCs and 31 h with LCs which is sufficient. This demonstrates nicely that the rf cavities have been specified sufficiently well for operation of a fully loaded ring.

Finally, to summarize these various cases Fig. 22 shows radiation losses and equilibrium emittance as a function of the number of installed pmuL in the otherwise bare lattice.

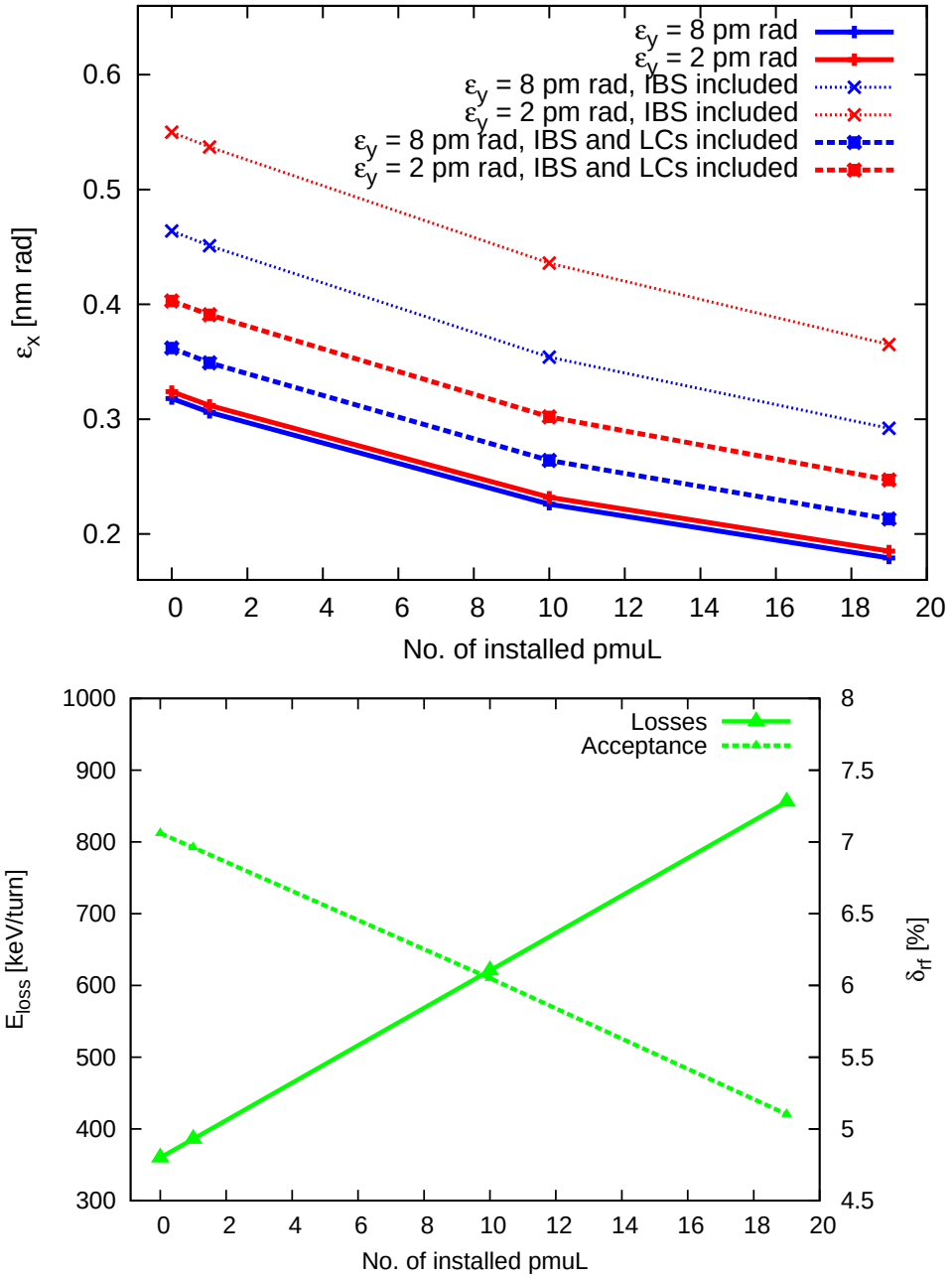

Figure 22: Emittance and radiation losses of the MAX IV 3 GeV storage ring for different numbers of installed pmuL. Beside the bare lattice emittance, the effect of emittance blowup from IBS, and the effect of tuning in the LCs ($\sigma_s = 50$ mm for all cases) is shown. For all cases the overall cavity voltage has been set to 1.8 MV.

7 Summary of Other Changes in the New Lattice

The following is a summary of further changes applied to branch 20101101 resulting in the new lattice branch 20110117.

- The pulsed sextupole magnet and dipole kicker for injection are now both included in the lattice and have a finite length. The PSM is 300 mm long, while 500 mm have been reserved for the dipole kicker.
- The horizontal and vertical pinger magnets have been included in the lattice. Their (preliminary) length has been set at 300 mm.
- The nomenclature in the lattice file has been updated.
- The PMDW now used in the lattice file is 4 m long. Instead of occupying four straights with four 2 m long devices, we now use only two straights to achieve the same amount of damping.

8 Current Lattice Files

Table 15 lists all current official lattice files [1] and what type of elements are included. The lattice files are human-readable and in Tracy-3 format. All lattice files contain BPMs and correctors (SOFB). Girder markers are also included.

Table 15: List of all current lattice files.

File name	Lattice contains
m4-20110117-420-bare.lat	Bare ring lattice, injection elements included
m4-20110117-420-2W.lat	2×4 m PMDW installed in otherwise bare ring
m4-20110117-420-10U.lat	10×3 m IVU installed in otherwise bare ring
m4-20110117-420-01pmuL.lat	1 pmuL installed in otherwise bare ring
m4-20110117-420-10pmuL.lat	10 pmuL installed in otherwise bare ring
m4-20110117-420-19pmuL.lat	19 pmuL installed, "fully loaded ring"

References

[1] The updated lattice files can be found at `http://www.maxlab.lu.se/node/999`

[2] L.-J. Lindgren, unpublished internal note.

[3] The MAX IV Detailed Design Report, available at http://www.maxlab.lu.se/node/1136

[4] E. Wallén, S.C. Leemann, "Strategy for Neutralizing the Impact of Insertion Devices on the MAX IV 3 GeV Ring", PAC'11, New York NY, USA, March 2011, TUP235.

[5] P. Elleaume O. Chubar and J. Chavanne, Journal of Synchrotron Radiation, 5:481, 1998.

[6] A. Streun, Momentum acceptance and Touschek lifetime, SLS Internal Note 18/97, http://ados.web.psi.ch/slsnotes/sls1897a.pdf.

[7] S.C. Leemann et al., Phys. Rev. ST Accel. Beams 12, 120701 (2009).